RHEOLOGY AND PHASE CHANGE OF POLYMERS AND VESICLES

ZHENG ZHANGFENG

(B. ENG., Tianjin University)

A THESIS SUBMITED

FOR THE DEGREE OF MASTER OF ENGINEERING

DEPARTMENT OF CHEMICAL AND BIOMOLECULAR ENGINEERING

NATIONAL UNIVERSITY OF SINGAPORE

2010

ACKNOWLEDGEMENT

I would like to express my sincere appreciation to my supervisor, A/Prof. Chen Shing Bor for his guidance, support and encouragement throughout my research work. His rigorous attitude towards research gives me a deep impression and benefits me a lot.

I would also like to express my thanks to all my labmates: Miss. Zhou Huai, Miss. Chieng Yu Yuan, Miss. Moe Sande, and Mr. Zhang Tao, for their great help. Thanks are extended to Ms. Jamie Siew Woon Chee for her assistance.

A special gratitude is given to my wife, Geng Bo. Her love and encouragement kept me going on. Many thanks go to my family members for their firm support during my study in Singapore.

Finally, I wish to thank the National University of Singapore for providing the financial support.

TABLE OF CONTENTS

SUMMARY

This thesis investigated interactions between polymers and vesicles, focusing on the electrostatic interactions and hydrophobic interactions. Systems examined experimentally included a polyelectrolyte with oppositely charged surfactant vesicles, and a hydrophobically modified polymer with the vesicles. Polymers employed were poly (acrylamide-co-diallyldimethylammonium chloride) (PADA), and 2-hydroxyethyl cellulose hydrophobically modified with hexadecyl groups (hmHEC) respectively. The vesicles were composed of an anionic surfactant sodium dodecyl benzenesulfonate (SDBS) and a zwitterionic surfactant lauryl sulfonate betaine (LSB). The experimental methodology was rheometry.

For pure PADA solutions, they showed a behavior of Newtonian fluid at low concentrations, while shear thinning took place at high concentrations. Intermolecular hydrogen bonds were the driving force for entanglements and network. Based on the distinct concentration dependence of zero-shear viscosity, three concentration regimes were identified: the dilute regime $C < C^*$(ca. 1wt %), the semidilute regime $C^* < C < C^{**}$ (ca. 3wt %), and the concentrated regime $C > C^{**}$. For PADA-SDBS/LSB vesicle mixture solutions, the rheological properties exhibited nonmonotonic functions of vesicle concentration. At low vesicle concentrations, zero-shear viscosity decreased with concentration, while it beccame increased at higher concentrations. According to the oscillatory shear results, both crossover modulus and apparent relaxation time decreased with the vesicle concentration at low vesicle concentrations. However, at higher vesicle concentrations, they increased. In addition, salt effect on viscosity was also investigated. The effect was pronounced for PADA-vesicle mixture solutions, but not significant for

pure PADA solutions.

For pure hmHEC solutions, shear thickening behavior was observed at intermediate concentrations and shear rates. Four concentration regimes were identified: the dilute regime (C<0.15wt %), the semidilute unentangled regime (0.15wt %< C<0.25wt %), the semidilute entangled regime (0.25wt %< C<0.4wt %), and the concentrated regime (C >0.4wt %). The four regimes showed distinct concentration dependences of zero-shear viscosity. For hmHEC-vesicle mixture solutions, the variation of rheological properties with vesicle concentration was not monotonic. The zero-shear viscosity was initially increased with vesicle concentration and reached the maximum at a certain concentration. Beyond the concentration, the viscosity was decreased with concentration. For the crossover modulus and apparent relaxation time, their trends were similar to that of the zero-shear viscosity. Strong gelation can take place for certain compositions.

NOMENCLATURE

Abbreviations	Description
Aerosol OT	Sodium bis(2-ethylhexyl) sulfosuccinate
CTAB	Cetyl trimethyl ammonium bromide
CTAT	Cetyl trimethyl ammonium tosylate
CDP	Cyclic di-*n*-dodecyl sodium phosphate
cryo-TEM	Cryogenic Transmission Electron Microscopy
DDAB	Didodecyl dimethyl ammonium bromide
DSC	Differential scanning calorimetry
DTAB	Dodecyl trimethyl ammonium bromide
DTAC	Dodecyltrimethylammonium chloride
hm-chitosan	Hydrophobically modified chitosan
hmHEC	Hydroxyethyl cellulose hydrophobically modified with hexadecyl groups
hmPEG	Hydrophobically modified polyethylene glycol
hmPSA	Hydrophobically modified poly (sodium acrylate)
JR400	Hydroxyethyl cellulose derivative with a charge concentration of 10 mM (1 wt% polymer)
LM200	Hydroxyethyl cellulose derivative with a charge concentration of 2 mM (1 wt% polymer) and 0.76% of hydrophobic modification.
LSB	Lauryl sulfonate betaine
NaCl	Sodium chloride
PADA	Poly (acrylamide-co-diallyldimethylammonium chloride)
PDADAMAC	Poly (diallyldimethylammoniumchloride)
PVP	Polyvinylpyrrolidone
SDBS	Sodium dodecyl benzenesulfonate
SDS	Sodium dodecylsulfate

Symbols

a	Head group area
C	Concentration
E_a	Activation energy
f	Frequency
f_c	Crossover frequency
G'	Storage modulus
G''	Loss modulus
G_∞	Plateau value of G' at high frequency
k	Boltzmann constant
l	Chain length of the hydrophobic group
n	Number of elastic active chains
P	Packing parameter
R	Gas constant
T	Temperature
t	Time
v	Volume of hydrocarbon tail of the surfactant

Greek Letters

γ	Shear strain
γ_0	Strain-amplitude
δ	Phase difference
η	Vicosity
η_0	Zero-viscosity

σ	Shear stress
σ_0	Stress-amplitude
τ	Relaxation time
ω	Angular frequency

LIST OF TABLES

LIST OF FIGURES

Chapter 1 INTRODUCTION

1.1 Background

Vesicles are self-closed bilayer structures formed in aqueous solution on the dispersion of certain amphiphilic molecules, such as surfactants, lipids, or block copolymers. (Kaler et al., 1989, Lasic, 1993, Discher and Eisenberg, 2002). The interior of the shell consists of the hydrophobic tails and the hydrophilic head groups are exposed to the aqueous solution on both surfaces of the bilayer. Vesicles are generally spherical and can be unilamellar, multilamellar, or even oligovesicular. Vesicles can be used to simulate the behavior of biological cells or membranes and hence have been the subject of intensive scientific research. More importantly, they also are of interest for many technological applications from drug delivery and controlled release to bioseparations and sensing (Lasic, 1993).

Lipid vesicles (liposomes) were discovered by Bangham (1965), and have received much attention since then. However, surfactant vesicles attracted intensive interest well after Kaler et al. (1989) prepared spontaneously formed and stable vesicles. So far, surfactant vesicles have been formed from a variety of surfactant mixtures in aqueous solutions. In recent years, spontaneously formed vesicles from a mixture of an anionic surfactant and a zwitterionic single-tailed surfactant have been reported (Zhai et al., 2001, 2005b).

Due to the mimicking of biological systems and technological applications in most industrial formulations, such as pharmaceutical and cosmetic formulations, interactions between polymers and vesicles are of interest. Many papers have made contributions in this field. The interactions can be one or combination of the following interactions: hydrophobic interactions, that is, the insertion of hydrophobic moieties in the polymer chain into the vesicle bilayer, and electrostatic interactions, i.e. Coulomb forces between charged polymers and vesicles. It should be noted that association between some polymers and vesicles is attributed to hydrogen bonds in some articles.

Two kinds of polymer are involved in this study: associative polymer and polyelectrolyte. Associative polymers generally are water-soluble polymers with hydrophobes attached to the main polymer backbone, either distributed randomly along the chain or at the ends of the backbone. Polyelectrolyte refers to a polymer with ionizable groups. In water these ionizable groups can dissociate, leaving charges on polymer chains and releasing counterions (Dobrynin and Rubinstein, 2005).

For mixtures of polymers and vesicles, one can either have a vesicle- or a polymer-centered view. One can focus on the polymer effect on vesicles, like vesicle disruption, shape change, or structural rearrangement in the vesicle bilayer. One can also emphasize how vesicles influence a polymer network, such as giving rise to a gel-like sample.

From the polymer-centered view, it is of interest to investigate phase behaviors and rheological properties of mixtures of polymers and vesicles.

1.2 Objectives

In this thesis, electrostatic interactions between a positively charged copolymer poly (acrylamide-co-diallyldimethylammonium chloride) (PADA) and oppositely charged surfactant vesicles composed of an anionic single-tailed surfactant sodium dodecyl benzenesulfonate (SDBS) and a zwitterionic single-tailed surfactant lauryl sulfonate betaine (LSB), and hydrophobic interactions between 2-hydroxyethyl cellulose hydrophobically modified with hexadecyl groups (hmHEC) and the surfactant vesicles were experimentally investigated.

For PADA-SDBS/LSB vesicle mixtures, specific objectives are as follows: to construct the phase map of the mixtures; to examine the rheological properties of pure PADA solutions; to identify PADA concentration regimes; to evaluate the temperature and salt effect on pure PADA solutions; to investigate vesicle effect on the rheological properties of PADA solutions; to study salt effect on the viscosity of the polymer-vesicle mixtures.

As to hmHEC-vesicle mixtures, the specific objectives include: to construct the phase map of the mixtures; to investigate the rheological properties of pure hmHEC solutions; to identify hmHEC concentration regimes; to examine vesicle effect on the rheological properties of hmHEC solutions; to study the transition from viscous solution to gel.

1.3 Thesis Organization

This thesis consists of five chapters. An introduction of the present study is described in Chapter 1. Chapter 2 gives a thorough literature review. Materials and methods employed in this research are given in Chapter 3. Chapter 4 presents the results obtained experimentally and the relevant discussions. The fifth and last chapter summarizes the conclusions that can be drawn from this investigation.

Chapter 2 LITERATURE REVIEW

2.1 Spontaneously formed vesicles

Vesicles can be formed through either input of external energy, such as sonication and filtration, or a spontaneous process without external energy imposed. Spontaneously formed vesicles refer to ones formed through a spontaneous process. It should be mentioned that it is necessary to apply some kind of agitation to make a sample homogenous during preparation. Here a brief review is given.

Self-assembly of surfactants in solution is spontaneous. Self-organized aggregates can have different morphology, depending on surfactant molecular structure. According to Israelachvili (1992), the aggregate morphology can be described by packing parameter *P:*

$$P = \frac{v}{la} \tag{2.1}$$

where v is volume of hydrocarbon tail of the surfactant, l is the chain length of the hydrophobic group, and a is the head group area. As known, hydrophobic effect is the driving force in association of surfactants. The head group area depends on two opposite forces: the hydrophobic attraction of the hydrocarbon chains in the hydrocarbon-water interface (Tanford, 1972), and the repulsion between neighboring head groups. The repulsive forces result from steric, ionic and hydrophilic repulsion. The hydrophobic attraction tends to lower the head group area, while the repulsion tends to raise it.

The packing parameter can be used to predict the morphology of surfactant aggregates. When the packing parameter is less than 1/3, spherical micelles are formed favorably. The formation of rodlike micelles is the most favorable if the packing parameter is between 1/3 and 1/2. A packing parameter between1/2 and 1 suggests that vesicles and flexible bilayers are formed, while flat bilayers are obtained if $P \approx 1$.

Any factors that alter two opposite forces may change the aggregate morphology. For ionic surfactants, ionic strength, pH, and temperature may modify the electrostatic repulsion between the head groups and hence the aggregate shape. Therefore, increasing the salt concentration of the aqueous solution of single-tailed ionic surfactants probably leads to compression of the head groups due to the reduced electrostatic repulsion. According to the equation 2.1, the packing parameter *P* increases with decreasing the head group area. The increase in *P* may result in the formation of vesicles (Zhai et al., 2005b).

By far, spontaneously formed vesicles have been prepared from various surfactant mixtures in aqueous solutions, like catanionic mixtures, cationic/cationic mixtures, nonionic/anionic mixtures, and zwitterionic/anionic mixtures. The catanionic vesicles are the most systems reported in literature. They include the following as example: DDAB/SDS (Kondo et al., 1995, Marques et al. 1998), CTAT/SDBS (Kaler et al. 1989, Yaacob and Bose, 1996, Salkar et al., 1998), DTAB/SDBS(Horrington et al., 1993, O'Connor et al., 1997, Meagher et.al, 1998), CTAB/ Sodium octyl sulfate (Yatchilla et al., 1996, Brasher et al., 1996).

Viseu et al.(2000) prepared the spontaneously formed vesicles from a mixtures of two cationic surfactants: DDAB and DTAC. For nonionic/anionic vesicles, Zhai et al.(2005a) published a paper on the spontaneously formed vesicles from octylphenoxypolyethoxyethanol (Triton X-100) and the double-tailed anionic surfactant Aerosol OT. Vesicles of a single-component Aerosol OT can be formed under the inducement of salt. However, the stability and the polydispersity of the vesicles composed of Triton X-100 and Aerosol OT are greatly enhanced. The formation and growth of the vesicle are controlled by salt concentrations. Without inducing salt, no vesicles are found in the aqueous solution. It seems that the mechanism of vesicle formation could be attributed to the compression of the head groups due to the reduced electrostatic repulsion by salt.

Zhai et al. (200l) reported the spontaneously formed vesicles from an anionic surfactant Aerosol OT and a zwitterionic surfactant LSB. They (2005b) also prepared another zwitterionic/anionic vesicles from LSB and SDBS. The single-tailed anionic surfactant SDBS can self-assemble spontaneously into vesicles just under inducement of salt. The addition of LSB makes the vesicles more stable, and improves the polydispersity of the vesicles. It is found that the vesicle size increases with the salt concentration, and is indpendent of the surfactant concentration at the same salinity. It is noteworthy that the polydispersity of the vesicles has a minmum when the molar ratio of SDBS to LSB is 7 to 3.

On spontaneous formation of vesicles, there are a few detailed reviews (Tondre and Caillet 2001, Marques et al., 2003, Šegota and Težak, 2006), to which interested readers can refer.

2.2 Polymer-vesicle systems

Vesicles could be composed of lipids or surfactants. For historical reasons, the lipid vesicles were firstly investigated, well before the surfactant vesicles attracted intensive interest. The surfactant vesicles did not receive much attention until the spontaneously formed vesicles were discovered. The field of lipid vesicles has traditionally been separated from that of surfactant vesicles in academic society. However, from the viewpoint of physical chemistry, association between polymers and lipid vesicles is more or less similar to that between polymers and surfactant vesicles. Here the association between polymers and surfactant vesicles is focused.

Association between polymers and surfactant vesicles has the following driving forces: electrostatic interactions and hydrophobic interactions. It should be noted that there are not any papers in literature, in which the association is attributed to hydrogen bonding, while for lipid vesicles there are some papers where association between polymers and lipid vesicles is ascribed to this mechanism. The electrostatic interactions are Coulomb forces between charged polymers and vesicles. The hydrophobic interactions are the insertion of the hydrophobic moieties of the polymer chain into the vesicle bilayer. Therefore, polymer can interact with surfactant vesicles through

electrostatic interactions, hydrophobic interactions, or both of them simultaneously. When there are only electrostatic interactions at play, polymers and vesicles should be oppositely charged for their association. When there are both electrostatic and hydrophobic interactions simultaneously, polymers can be either oppositely or similarly charged with vesicles if hydrophobes are long enough.

Hydrophobic interactions can result in the association between vesicles, whether charged or not, and polymers with hydrophobic modification and no charges. Polymers with charges but no hydrophobic modification can only interact with oppositely charged vesicles. However, polymers with charges and hydrophobic modification can interact with similarly charged vesicles. When the hydrophobes are long enough, the hydrophobic interactions could overcome electrostatic repulsion.

In literature, there are a few papers to investigate the association between polymers and vesicles through electrostatic interactions alone (Regev et al., 1999, Marques et al., 1999, Antunes et al., 2004, Zhai et al., 2004, Antunes et al., 2007, Dew et al., 2009, and Lin et al., 2009). The polymers used include cationic JR400 and PVP. PVP tends to be positively charged in aqueous solution. The vesicles are negatively charged catanionic SDS/DDAB vesicles, SDS/alprenolol vesicles, and SDBS / CTAB vesicles.

There exist studies in literature to investigate association polymers and vesicles associate through only hydrophobic interactions. Loyen et al. (1995) investigated the association between hydrophobically modified poly (sodium acrylate) (hmPSA) and a series of nonionic surfactants of dodecyl ethers of oligothylene glycol ($C_{12}E_3$, $C_{12}E_4$, and

$C_{12}E_5$). The association between poly (acrylamide-co-n-dodecyl methacrylate) and CDP vesicles or DDAB vesicles was examined by Kevelam et al. (1996). Meier et al. (1996) studied association between hydrophobically modified poly (oxyethylene) with cholesterol and vesicles composed of DODAC or biological cells. Lee et al. (2005) examined association between hm-chitosan and SDBS/CTAT vesicles. The association between hmPEG and SDS/DDAB cationic vesicles was investigated (Medronho et al., 2006). Santos et al. (2008) examined association between hmPEG and non-ionic vesicles consisting of tetraethylene glycol monododecyl ether ($C_{12}E_4$). Lin et al. (2009) studied association Plus 300 and two catanionic vesicles, SDS/ hexadecyltrimethylammonium bromide vesicles and sodium tetradecylsulfate/ tetradecyltrimethylammonium bromide vesicles. Plus 300 is a hydrophobically modified HEC.

The association between hydrophobically modified polyelectrolyte and oppositely charged vesicles has been reported (Regev et al., 1999, Marques et al., 1999, Antunes et al., 2004, Dew et al., 2009, and Lin et al., 2009). The polymer used is cationic LM200, and the vesicles are catanionic. Kevelam et al. (1996) examined the interactions between poly (sodium acrylate-co-n-alkyl methacrylate) and CDP or DDAB vesicles, where n-akkyl is C_9H_{19}, $C_{12}H_{25}$, or $C_{18}H_{37}$. The association between modified polyelectrolyte and similarly charged vesicles has also been published. Ashbaugh et al. (2002) studied interactions between hmPSA and negatively charged vesicles composed of SDS/DDAB and SDBS/CTAT.

2.2.1 Phase behaviors of polymer-vesicle mixtures

Polymer-vesicle mixtures can show either miscibility or phase separation, depending on the polymer and vesicle concentration. Miscibility can be reflected in the form of either solution or gel.

For mixtures of polyelectrolyte without hydrophobic modification and oppositely charged vesicles, three typical behaviors can be observed: single-phase solution, phase separation (or precipitation), and gel (Regev et al., 1999, and Marques et al., 1999). This trend has been verified for JR 400 and negatively charged catanionic SDS/DDAB vesicles. However, Dew et al. (2009) found that mixtures of JR400 and catanionic SDS/alprenolol vesicles did not lead to gel formation. It appears that the constituting species for the vesicles play an important role in the phase behavior of the mixtures.

For the mixtures of hydrophobically modified polymers and vesicles, Regev et al. (1999) and Marques et al. (1999) observed the same phases as those for mixtures of polyelectrolyte without hydrophobic modification and oppositely charged vesicles. The systems investigated were mixtures of LM200 and oppositely charged catanionic SDS/DDAB vesicles. This is probably traced to the fact that the electrostatic interactions along with the hydrophobic interactions are the driving force for the association. For hmPEG and SDS/DDAB cationic vesicles, the aforementioned three phase behaviors also were observed (Medronho et al., 2006). The phase separation is associative in nature. One phase is rich in the polymer and vesicles, while the other is a water-rich phase. The associative phase separation was confirmed by cryo-TEM, H-NMR and cloud point

determinations (Medronho et al., 2006). For mixtures of hmPEG and non-ionic vesicles composed of tetraethylene glycol monododecyl ether ($C_{12}E_4$), Santos et al. (2008) found a similar trend. It seemed that for mixtures of vesicles and hydrophobically modified polymers, the phase behavior is dependent primarily on the polymers.

2.2.2 Network and rheology of polymer-vesicle mixtures

The interactions between hydrophobically modified polymers and vesicles can give rise to polymer-vesicles networks, leading to an elastic gel. Loyen et al. (1995) investigated the association between hmPSA and vesicles composed of ionic surfactant $C_{12}E_3$, $C_{12}E_4$, or $C_{12}E_5$. They found that the rheological properties of the polymer-surfactant mixtures strongly depended on the nature of the aggregates, micelles or vesicles. With increasing temperature, a sharp increase in viscosity and gelation was observed for some mixtures. The authors also found that the temperature of thermal gelation was correlated to a micelle to vesicle transition of the surfactant. Meier et al. (1996) demonstrated that hydrophobically modified poly (oxyethylene) was able to interconnect dimethyldioctadecylammonium chloride vesicles and living cells, leading to gel formation of vesicles and polymer. Ashbaugh et al. (2002) exhibited that stable vesicle gels can be formed for certain compositions of negatively charged vesicles (SDS/DDAB or SDBS/CTAT) and similarly charged hmPSA. It seemed that hydrophobic interactions were strong enough to overcome the electrostatic repulsions. According to results of rheological measurements, the gels exhibited a transition from a Maxwell fluid to a critical gel to an elastic solid with either rising vesicle and /or polymer

concentration. When the polymer concentration is fixed, solutions at low surfactant concentrations are nearly Maxwellian with power-law exponents of 2.1 and 0.99 for the frequency dependence of storage and loss moduli, respectively. At intermediate surfactant concentrations, the samples behave like a non-Maxwellian fluid with loss modulus still greater than storage modulus over the range of frequency and the exponents less than their idealized Maxwell values. At larger surfactant concentrations, a critical gel is obtained with storage modulus equal to loss modulus over a broad range of frequency. Beyond the critical gel concentration, storage modulus exceeds loss modulus over the range of frequency and the storage modulus is increasingly independent of frequency, indicating the formation of strong elastic gels. An elastic gel can be formed by adding hm-chitosan to the SDBS/CTAT vesicle solution (Lee et al., 2005). The authors proposed a gel structure where the vesicles were bridged by the polymer chains into a three-dimensional network. The hydrophobes inserted into the vesicle bilayer, and hence vesicles served as multifunctional junctions. In addition, they reported that gel formation did not take place for the native chitosan without hydrophobes. Besides, adding the hm-chitosan to a micelle solution did not lead to gel formation. This is probably due to the high volume fraction of vesicles, in contrast to micelles.

Mixtures of polyelectrolyte and oppositely charged vesicles can also give rise to gel formation (Regev et al., 1999, and Marques et al., 1999). The vesicles were probably bridged by the polymer chains into a three-dimensional network through Coulomb forces. Polymer charge density and hydrophobic group length are important factors for the type of network.

Antunes et al. (2004) investigated samples composed of negatively charge SDS/DDAB vesicles and two oppositely charged polymers within the gel region by rheological measurements. These two polymers are JR400 and LM200, JR400 having higher charge density than LM200 with hydrophobes. For LM200-vesicle mixtures, a typical viscoelastic behavior was observed. At low frequencies there was a liquid-like response with loss modulus larger than storage modulus, while at high frequencies a solid-like response resulted with storage modulus exceeding loss modulus. For JR400-vesicle mixtures, storage modulus exceeded loss modulus over the whole frequency range accessible. It should be noted that LM200-vesicle samples have larger storage moduli than the JR400-vesicle system. According to the rheological properties, a higher charge density seemed to result in longer lifetime of cross-links, while the hydrophobic groups probably led to a higher number of cross-links.

The viscosity of mixtures of polyelectrolyte JR400 and oppositely charged SDS/DDAB vesicles exhibited a strong dependence on temperature (Antunes et al., 2007). The viscosity of JR400-vesicle mixtures decreased with temperature, with an inflection point at 15℃, above which the temperature dependence of the viscosity was weaker. The authors also found that according to DSC results, the temperature 15℃ corresponded to the chain melting temperature of the vesicles. The temperature dependence of the viscosity was probably correlated with the surfactant flexibility at molecular level. When the vesicles were in a fluid state above the chain melting temperature T_m, the surfactants had disordered alkyl chains and the vesicles exhibited a typical spheroidal shape. Below T_m, the vesicle bilayer was less flexible, probably

inducing a shape change, like the formation of faceted vesicles, and hence leading to a higher viscosity.

2.2.3 Vesicle microstructure changes

When polymers associate with vesicles, the former probably affect the microstructure of the latter. Regev et al. (1999) and Marques et al. (1999) investigated the association of JR400 and SDS/DDAB vesicles, and that of LM200 and SDS/DDAB vesicles. In the solution phase, faceted vesicles and disklike aggregates were observed for the JR400-vesicle systems, while for the LM200-vesicle systems, besides faceted vesicles, clusters of vesicles and other bilayer structures were found. The clusters of vesicles probably resulted from the vesicles bridging by LM200 chains through hydrophobes. In the gel phase of JR400, disklike aggregates, vesicles, and membrane fragments were also observed. Without polyelectrolyte, the repulsive forces make the vesicles stable. Addition of polyelectrolyte, however, may result in a decrease in vesicle stability due to the screening of the repulsions by the polyelectrolyte. This leads to flocculation of the aggregates. The adsorption of the polyelectrolyte on the surface of vesicles may also cause changes in the vesicle microstructure. The faceted vesicles probably result from the polymer adsorption on the surface of vesicles. Antunes et al. (2004) further investigated the microstructures of polymer-vesicle mixtures. For LM200 the aggregates remained largely in the form of faceted vesicles and globular vesicles. For JR400, however, the aggregate structure changed in different ways: the shape of the vesicles altered from a globular to a faceted form; and there was holey vesicles leading to

considerable vesicle disruption and to planar bilayer, disklike aggregates. The formation of faceted vesicles was attributable to a crystallization of the bilayer in vesicles. It can be inferred that LM200 can better stabilize the vesicles, whereas JR400 interacts so strongly with the bilayer due to electrostatic interactions that the vesicles are perturbed and even disrupted.

Antunes et al. (2007) published another paper on the same systems in which mechanisms behind the formation of the faceted vesicles were focused. They found that in the gel phase, LM200 enhanced the chain melting temperature of the vesicles, while JR400 lowered it. The rheological results showed that for both polymer-vesicle systems, the viscosity had an inflection point at the chain melting temperature, and the measured relaxation times were much higher below the melting temperature for LM200. According to the vesicle imaging by cryo-TEM, the neat vesicles and the polymer-bond vesicles were faceted below the chain melting temperature, that is, the surfactant chain crystallized. Above the temperature, the neat and the LM200-bound vesicles were of spheroidal shape, while the JR400-bound vesicles were still of deformed faceted shape. These results from DSC, cryo-TEM and rheology suggested that there were different mechanisms behind the faceting, depending on charge density and hydrophobic modification. For LM200 with a lower charge density and hydrophobes, a crystallization-segregation mechanism was proposed, whereas for JR400 with more densely charge and without hydrophobes, a charge polarization-lateral segregation mechanism was offered.

In addition, Lee et al. (2005) found that the vesicles were still intact within the gel of hm-chitosan and SDBS/CTAT vesicles by small-angle neutron scattering. However, the vesicles may re-organize into smaller vesicles upon adding hm-chitosan.

Chapter 3 MATERIALS AND METHODS

3.1 Principles of experimental methods

Rheology is defined as the science of flow and deformation of matter. Rheological measurements are very useful. The microstructure in materials can be correlated with these measurements, which are typically carried out under steady or oscillatory dynamic shear. For steady shear measurements which correspond to relatively high deformations, a constant shear stress (or shear rate) is applied to a sample, and shear rate (or shear stress) is recorded in response. Viscosity is defined as the ratio of shear stress to shear rate. A plot of viscosity versus shear stress (or shear rate) is called the flow curve of the sample.

For oscillatory dynamic shear measurements, a sinusoidal strain γ is applied to a sample:

$$\gamma = \gamma_0 \sin(\omega t) \tag{3.1}$$

where γ_0 is the strain-amplitude, that is, the maximum applied deformation, and ω is the angular frequency of the oscillations. The sample responds in a sinusoidal stress σ which has a phase difference δ with respect to the strain:

$$\sigma = \sigma_0 \sin(\omega t + \delta) \tag{3.2}$$

where σ_0 is the stress-amplitude.

The sinusoidally varying stress can be decomposed into two components, one in phase with the strain and the other in phase with the rate of strain:

$$\sigma = G'\gamma_0 \sin(\omega t) + G''\gamma_0 \cos(\omega t) \tag{3.3}$$

where *G'* is the elastic or storage modulus and *G''* is the viscous or loss modulus. The elastic modulus *G'* provides information about the elastic nature of the material. *G'* is also called the storage modulus because elastic behavior represents the storage of deformational energy. The viscous modulus *G''*, on the other hand, characterizes the viscous nature of the material. *G''* is also referred to as the loss modulus because viscous deformation results in energy dissipation.

Dynamic rheological measurements must be conducted in the linear viscoelastic regime. "If the deformation is small or applied sufficiently slowly, the molecular arrangements are never far from equilibrium. The mechanical response is then just a reflection of dynamic processes at the molecular level which go on constantly, even for a system at equilibrium. This is the domain of linear viscoelasticity. The magnitudes of stress and strain are related linearly, and the behavior for any liquid is completely described by a single function of time." (Mark et al., 1984) Over this regime, the storage and loss moduli will be functions only of the oscillation frequency ω. A log-log plot of the moduli dependence on frequency, i.e. *G' (ω)* and *G'' (ω)*, is referred as to the frequency spectrum or dynamic mechanical spectrum which reflects the microstructure.

Therefore, we can correlate measurements under steady shear to flow-induced changes in microstructures, and dynamic rheological measurements to static microstructures.

3.2 Materials

A 10 wt% solution of poly (acrylamide-co-diallyldimethylammonium chloride) (PADA) in water from Aldrich was used as received. According to the manufacturer, the copolymer has an average molecular weight Mw≈250,000 g/mol with ~55 wt% acrylamide and ~ 45 wt % diallyldimethylammonium chlorides. A 20wt % solution of Poly (diallyldimethylammoniumchloride) (PDADAMAC) in water from Aldrich was used as supplied. According to the manufacturer, the polymer has an average molecular weight Mw≈ 400,000-500,000 g/mol. 2-hydroxyethyl cellulose hydrophobically modified with hexadecyl groups (hmHEC) from Aldrich was used as received. According to the manufacturer, the polymer has an average molecular weight Mw= 560, 000 g/mol with the molar and degree substitutions being 2.7-3.4 and 2.0, respectively. The H^1NMR result showed that on average, each molecule possesses 10 hydrophobes randomly distributed along its backbone (Zhao and Chen, 2007). The anionic single-tailed surfactant sodium dodecyl benzenesulfonate (SDBS), purchased from Aldrich, was purified by means of recrystallization before used. The zwitterionic single-tailed surfactant lauryl sulfonate betaine (LSB) from Fluka was used as supplied in this study. Deionized water that had been further purified though a Millipore MIlliQ purification system and had resistivity of 18.2 MΩ cm was used. Sodium chloride from BDH

Laboratory Supplies is of analytical grade. The specifications of materials are listed in Table 3.1-3.3.

Table3.1Specifications of the polymers used

Chemicals	Poly (acrylamide-co-diallyldimethylammonium chloride)
Molecular structure	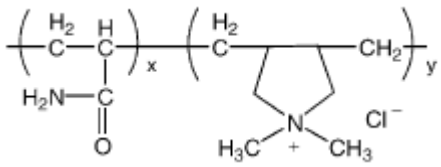
Molecular weight(g/mole)	≈250 000
Sources	Aldrich
Chemicals	Poly (diallyldimethylammoniumchloride)
Molecular structure	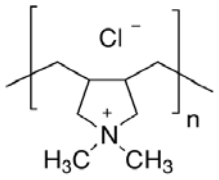
Molecular weight(g/mole)	≈400, 000-500,000
Sources	Aldrich
Chemicals	2-Hydroxyethyl cellulose hydrophobically modified
Molecular structure	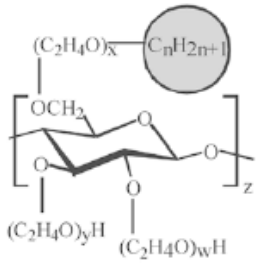 hmHEC n=16
Molecular weight(g/mole)	≈560, 000
Sources	Aldrich

Table3.2 Specifications of the surfactants used

Chemicals	Molecular formula	Molecular weight (g/mole)	Sources
Sodium dodecyl benzenesulfonate, SDBS	$C_{18}H_{29}SO_3Na$	348.48	Aldrich
Lauryl sulfonate betaine,LSB	$C_{17}H_{37}SO_3N$ 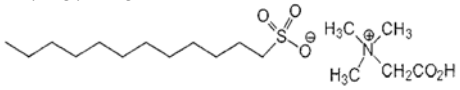	335.55	Fluka

Table3.3 Specifications of the salt used

Chemicals	Molecular formula	Molecular weight (g/mole)	Sources
Sodium chloride	NaCl	58.44	BDH

3.3 Experimental Methods and Procedures

3.3.1 Sample preparation

3.3.1.1 Purification of SDBS

SDBS was recrystallized before used. SDBS was firstly dissolved in methanol at 50°C. After dissolving, the resultant mixture was subsequently filtered. Then the filtrate was mixed with deionized water at the volume ratio 10:1. Finally, the solution was evaporated at 70°C until solvent was removed completely.

3.3.1.2 Preparation of surfactant vesicles

SDBS (or LSB) stock solutions were prepared by dissolving a precise amount of SDBS (or LSB) in deionized water. Stock solutions were filtered through 0.22μm filter

prior to preparing vesicles. Stock solutions of anionic and zwitterionic surfactant were mixed at desired molar ratio. In this study, the molar ratio of SDBS to LSB is 7 to 3. Vesicles were prepared by adding a precise amount of solid sodium chloride into the stock solution under brief vortex mixing. The sample was kept at rest for at least 2 hours for equilibrium before used.

3.3.1.3 Preparation of polymer-vesicle mixtures

The desired amount of vesicle stock solution was added into the polymer solutions at correct concentrations, and the mixtures were magnetically stirred for at least 2 hours at room temperature. Samples were stored at 4°C for at least 24 hours for full hydration and interaction.

3.3.2 Phase characterization

The phase boundary was evaluated by visual examination and tube inversion.

All the samples investigated contain 0.02M NaCl, unless otherwise stated.

3.4 Measurements

Rheological measurements were performed by using a Haake RS600 rheometer with a Haake Universal Temperature Controller. A cone-and-plate geometry of 60-mm diameter and a 4° cone angle was employed. The controlled stress test mode was applied to register the flow curves. Prior to frequency sweeps at a constant strain, a strain sweep measurement was carried out at a frequency of 1Hz to ensure that the tests were conducted in the linear viscoelastic regime with a large enough strain to minimize instrumental noise. After loading, each sample was allowed to be at rest for 10min before measurement to eliminate the mechanical history.

All measurements were carried out at 25℃, unless otherwise stated.

Chapter 4 RESULTS AND DISCUSSION

4.1 PADA-SDBS/LSB vesicles systems

4.1.1 Phase behaviors of mixtures of PADA and vesicles

Table 4.1: Phase behaviors of PADA mixed with SDBS/LSB vesicles

Conc. / PADA [wt%]	1	3	5	7	9
0mM	●	●	●	●	●
1mM	●	●	●	●	●
3mM	■	●	●	●	●
5mM	■	■	●	●	—
7mM	■	■	●	●	—
9mM	■	■	■	●	—

Black circles represent a single-phase solution. Black rectangles signify phase separation (precipitation). Black bars indicate that the mixtures are not investigated. All samples were prepared from 10wt% PADA stock solution and vesicle stock solutions.

Polymer-vesicle mixtures from PADA in different concentration regimes and vesicles at various concentrations were visually examined to construct the phase map. In this study, two typical behaviors, that is, a single-phase solution, and a phase separation (precipitation), were observed. Samples were stored for 3 days for full interactions and equilibrium before phase behaviors were identified by visual examination. For Table 4.1 shows the phase behaviors of PADA-SDBS/LSB vesicle mixtures obtained visually. It should be noted that for comparison, the phase behaviors of the pure PDAD in water at various concentrations were also given.

Upon the addition of negatively charged surfactant vesicles into the oppositely charged polyelectrolyte PDAD solution, the polyelectrolyte may adsorb on the vesicle surface due to electrostatic interactions. The surface charges of the vesicles would be gradually neutralized, and even the vesicles would be overcompensated, leading to charge inversion. Phase behaviors of the mixtures were dependent on the vesicle/polyelectrolyte charge ratio. As approaching to the isoelectric condition, aggregates became lager and larger. Precipitation probably occurred around the isoelectric point due to reduced repulsions between the aggregates.

4.1.2 Pure PADA solutions

4.1.2.1 General observations

Figure 4.1 shows typical shear stress dependences of the viscosity for pure PADA solutions. The general flow behavior is that at low shear stress, the solution is Newtonian, with the viscosity independent of shear stress, and above a certain critical shear stress, the viscosity decreases, showing a shear-thinning behavior. PADA is a copolymer composed of two monomers, acrylamide and diallyldimethylammonium chloride. For comparison, steady state shear flow experiments were carried out for PDADMAC. The results were presented in Figure 4.2. The viscosity is almost independent of shear stress. It seems that this cationic homopolymer solution is unentangled. In contrast, the copolymer PADA has much higher viscosity. The zero-shear viscosity of 7wt% PADA solution is 54 times larger than that of PDADMAC. The observation suggests that acrylamide plays a crucial role in the viscosity of PADA solutions. Due to the presence of the carbamoyl side group in acrylamide, PADA molecules can form intramolecular and intermolecular hydrogen bonds (Kulicke and Porter, 1980, and Kulicke and Kniewske, 1981). The intermolecular hydrogen bonds can act as cross-links or junctions of a network in polymer solutions, facilitating entanglements. Therefore the system can form a three-dimensional network. The viscosity would increase rapidly as the network structure develops. Compared to PADA, PDADMAC probably can not form a network structure due to strong electrostatic repulsions between monomers.

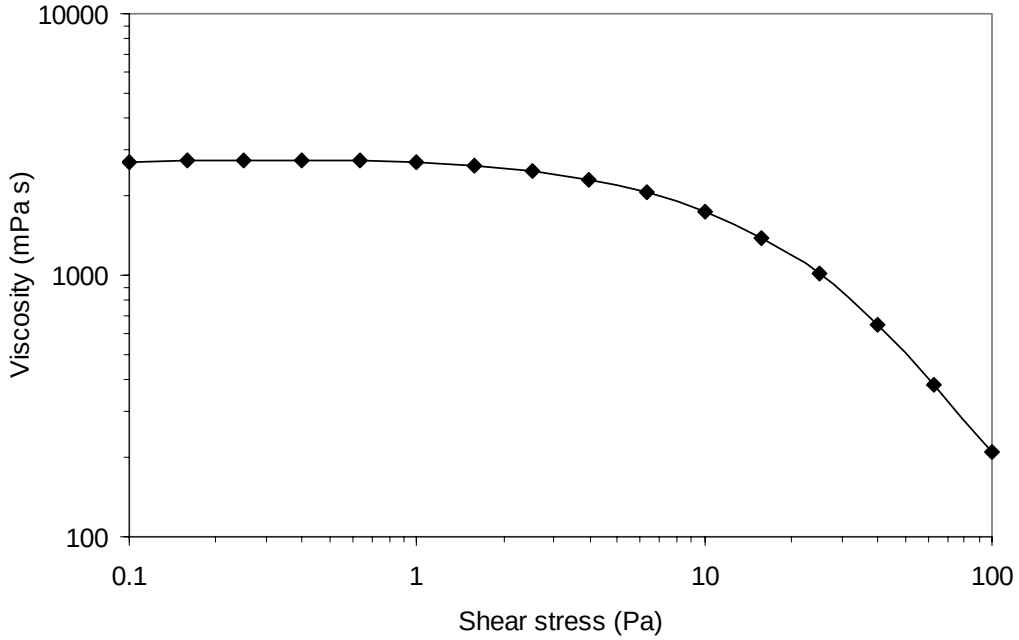

Figure 4.1: Shear stress dependence of the viscosity for 7wt% PADA solution

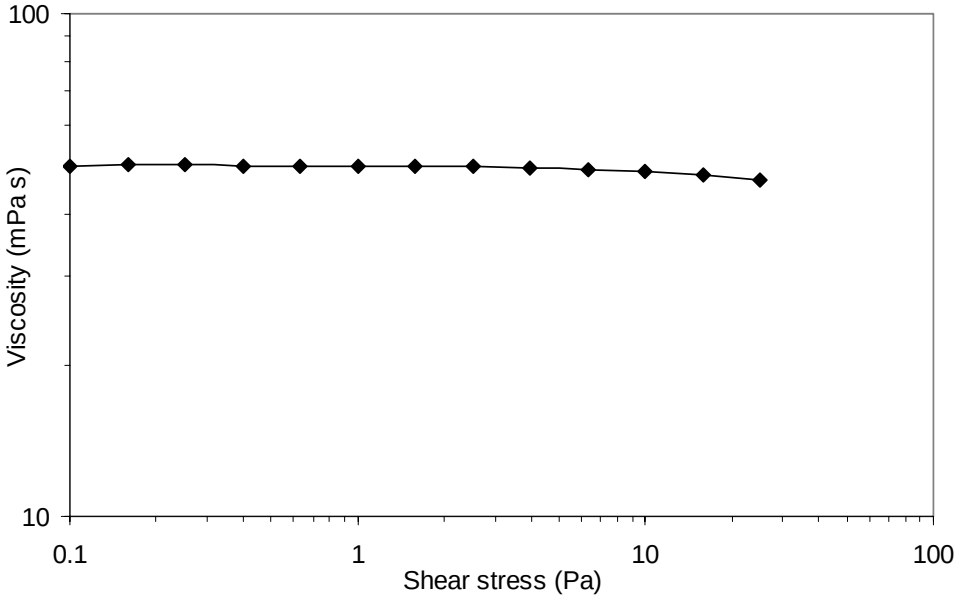

Figure 4.2: Viscosity of 7wt% PDADMAC solution as a function of shear stress

The decrease in the viscosity at higher shear stress, that is, shear thinning, as shown in Figure 4.1 is probably traced to the gradual breaking down of cross-links (intermolecular hydrogen bonds or mechanic entanglements) under strong shear. It should be noted that the repulsive forces between cationic monomers do not promote the network formation.

Typical frequency dependence of storage modulus *G'* and loss modulus *G''* for 7wt% PADA solution was shown in Figure 4.3. It can be seen that at low frequency, a viscous response was observed with *G'* less than *G''*, while *G'* increases to cross *G''* each other at relatively higher frequency. Beyond the crossover frequency, *G'* exceeds *G''*, indicating that the elastic response dominated over the viscous one. According to the dynamic behavior, the copolymer solution became more viscoelastic at higher frequency. This is a typical response of a cross-linked polymer network.

To analyze the dynamic data, a one-mode Maxwell model is tested. In this model, the storage modulus *G'* and loss modulus *G''* can be expressed as

$$G'(\omega) = G_{\infty} \frac{\omega^2 \tau^2}{1 + \omega^2 \tau^2} \tag{4.1}$$

$$G''(\omega) = G_{\infty} \frac{\omega \tau}{1 + \omega^2 \tau^2} \tag{4.2}$$

where G_{∞} is the plateau value of *G'* at high frequency, ω is the angular frequency, and τ is the relaxation time. Based on these two equations, one can obtain the following relationship

$$G''^2 = G'(G_\infty - G') \tag{4.3}$$

which can be rewritten as

$$\log(G'') = 0.5\log(G') + 0.5\log(G_\infty - G') \tag{4.4}$$

Provided *G'* much less than G_∞, one can draw a conclusion that for a single-mode Maxwell model, the relation between storage modulus and loss modulus in a log-log plot is linear, with a slope of 0.5. If the slope is different from 0.5, the system will likely possess a distribution of relaxation times.

Figure 4.4 shows *G''* against *G'* for of 7wt%PADA solution. According to the data, the slope of the fitting line is 0.64, not 0.5. This means that the system can not be fitted to a single-mode Maxwell model. The deviation is probably attributed to the system with a number of relaxation times.

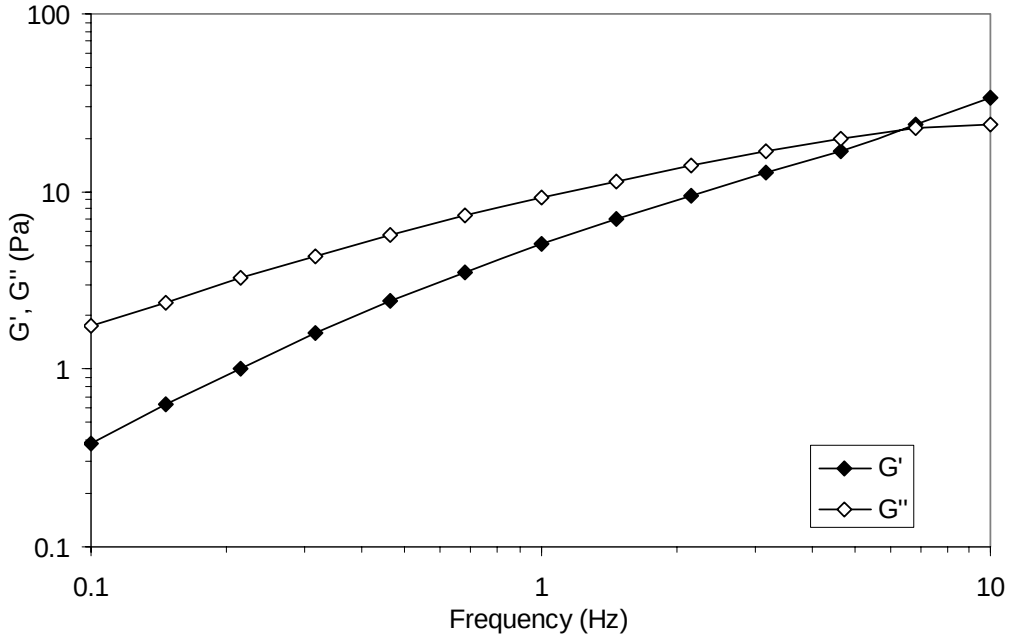

Figure 4.3: Frequency dependence of the storage and loss moduli of 7wt%PADA solution

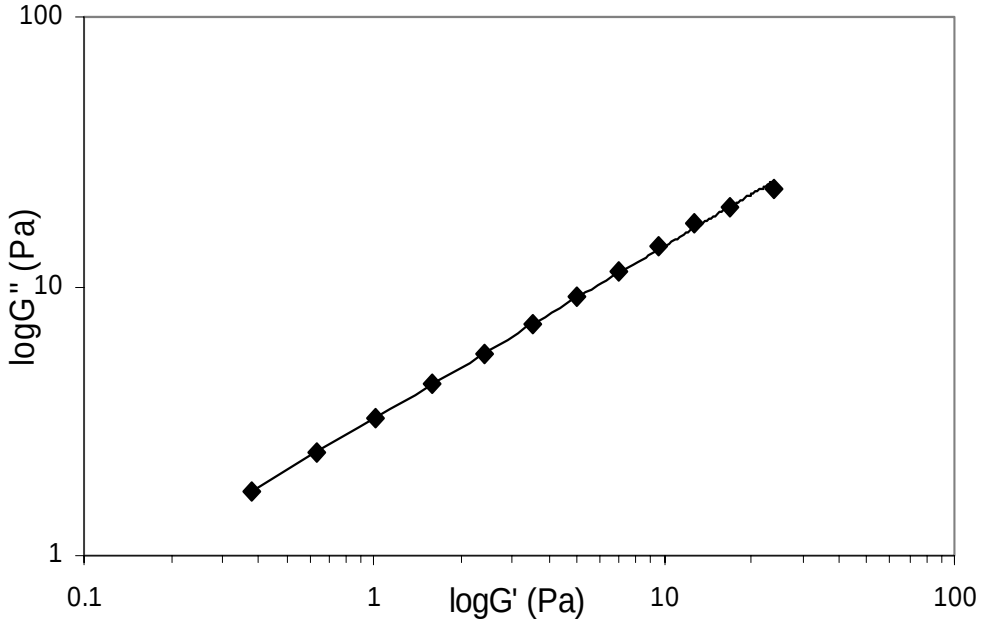

Figure 4.4: Log-log plot of *G''* versus *G'* for of 7wt%PADA solution

4.1.2.2 Concentration regimes

It is important to identify the different concentration regimes of PADA solutions prior to discussion on the linear and non-linear rheological properties. States of solutions will give us information on polymer molecules in solutions. Three distinct regimes of PADA solutions should be taken into account: dilute solution, semidilute solution, and concentrated entangled solution. Steady state shear experiments allow one determine these as illustrated in Figures 4.5 and 4.6.

Figure 4.5 shows the flow curves of PADA solutions at various concentrations. The flow behaviors change with concentration. At low concentrations, the system is nearly Newtonian, while the classical shear-thinning takes place at higher concentrations. Figure 4.6 presents the zero-shear viscosity as a function of PADA concentration. One can see that there are different scaling behaviors in different concentration regimes as described below.

(i) Dilute regime $C < C^*$

C* is the overlap concentration (ca. 1wt %). It is seen that the viscosity of PADA solutions is quite low, only a few times larger than that of water, until the polymer concentration reaches ca. 1wt%. Beyond C* a fast increase in the viscosity is observed. It is probably attributable to the transition from a dilute to a semidilute regime. The polymer molecules start to entangle with each other. In the dilute regime, the rheological behaviors of the solution are governed by individual polymer molecules. Polymer coils

are almost isolated from one another and hence the solution is almost Newtonian. The viscosity increases almost linearly with polymer concentration. It is noteworthy that both electrostatic interactions and intramolecular hydrogen bonds contribute to the viscosity. The repulsion forces tend to extend the chains, while the hydrogen bonds likely contract the chains.

(ii) Semidilute regime C* < C < C**

C** is ca. 3wt %. Beyond C*, the curve of concentration dependence of the zero-shear viscosity gives a different scaling behavior, $\eta_0 \sim C^{2.1}$, as shown in Figure 4.6. In the semidilute regime, entanglements become elastically effective. The intermolecular hydrogen bonds form and become strong driving forces for entanglements and association, whereas the electrostatic repulsive forces resist entanglements. However, the hydrogen bonds dominate over the repulsive forces. It seems that it is impossible to distinguish between cross-links caused by mechanical entanglements or by intermolecular hydrogen bonds.

(iii) Concentrated regime C >C**

In this regime, the zero shear viscosity scales as $\eta_0 \sim C^{4.26}$. It seems that the number of cross-links strongly increases with the concentration, and hence the viscosity rises with a higher exponent.

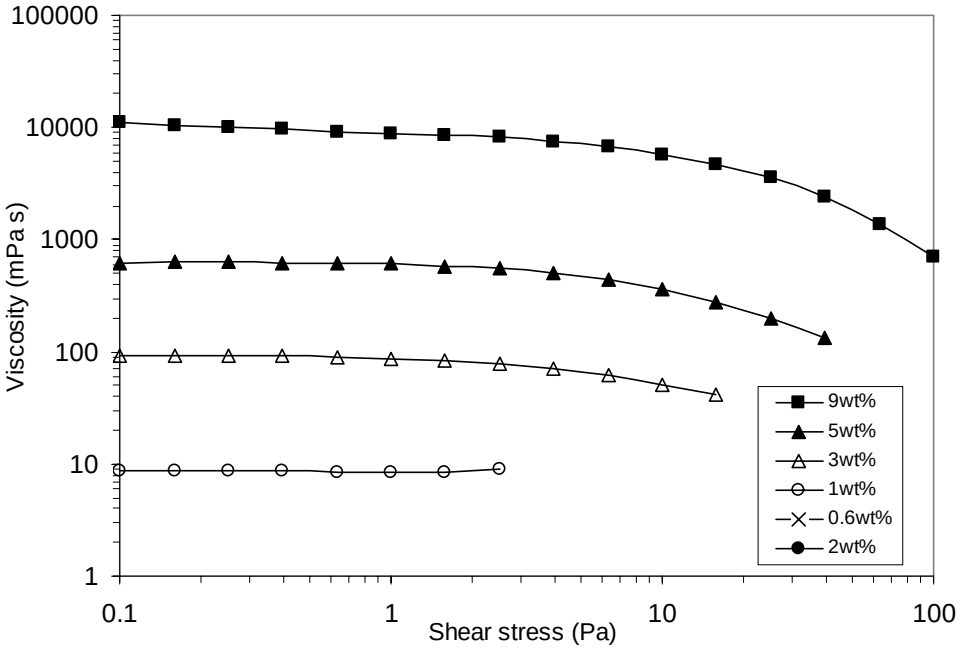

Figure 4.5: Viscosity versus shear stress for PADA solutions at various concentrations

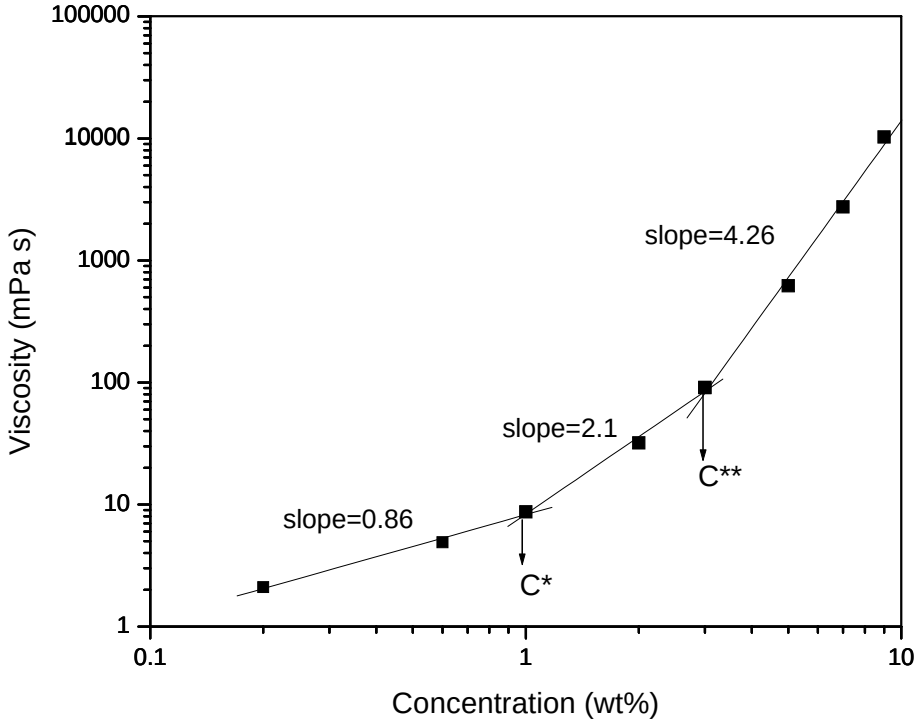

Figure 4.6: Concentration dependence of the zero-viscosity for PADA solutions

4.1.2.3 Influence of temperature

Figure 4.7 shows the shear stress dependences of the viscosity for 7wt% PADA solution at varying temperatures. One can see that the viscosity decreases with increasing temperature. This is typical temperature dependence often observed for polymers. To explain this behavior, one can use the following approximation:

$$\eta_0 \cong G_\infty \tau \tag{4.5}$$

where η_0 is the viscosity at the Newtonian plateau and τ is a characteristic relaxation time (Doi et al., 1986). Since the topology of the system is not altered much in temperature range studied, the temperature effect on the plateau modulus $G_\infty \cong nkT$ (n is the number of elastic active chains) should be weak (Ferry et al, 1980). To the contrary, the relaxation time may have an Arrhenius dependence on temperature

$$\tau \propto \exp(E_a / RT) \tag{4.6}$$

where E_a is activation energy. From the above relations, one can find that the zero-shear viscosity decreases with temperature as long as the activation energy is greater than RT. Figure 4.8 gives an Arrhenius plot for 7wt% PADA solution. The activation energy E_a is estimated to be around 13 kJ/mol (>RT). The energy is related to the disruption of a cross-link, hydrogen bond or mechanical entanglement. This energy is less than the strength of hydrogen bonds 21kJ/mol, probably attributable to the electrostatic repulsion between cationic monomers.

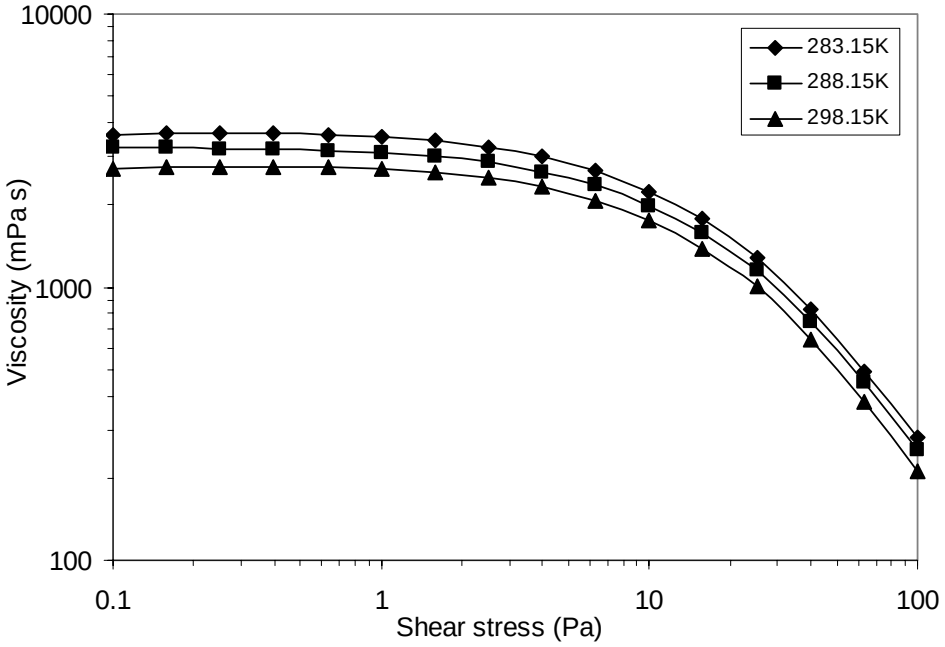

Figure 4.7: Stress dependence of viscosity of 7wt% PADA at varying temperatures

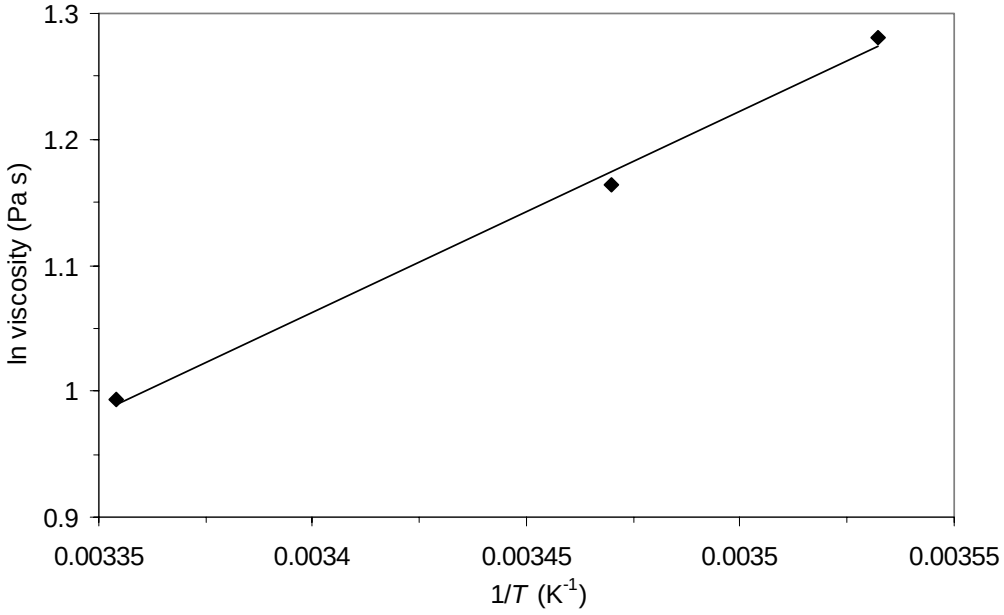

Figure 4.8: An Arrhenius plot of the zero-shear viscosity as a function of 1/*T* for 7wt% PADA

4.1.2.4 The effect of salt

The salt effect on the flow curve is shown in Figure 4.9, which plots the viscosity versus shear stress for 7wt% PADA solution at varying salt concentrations. It is seen that the salt concentration had no pronounced effect on the flow curve. The zero-shear viscosity only altered a little.

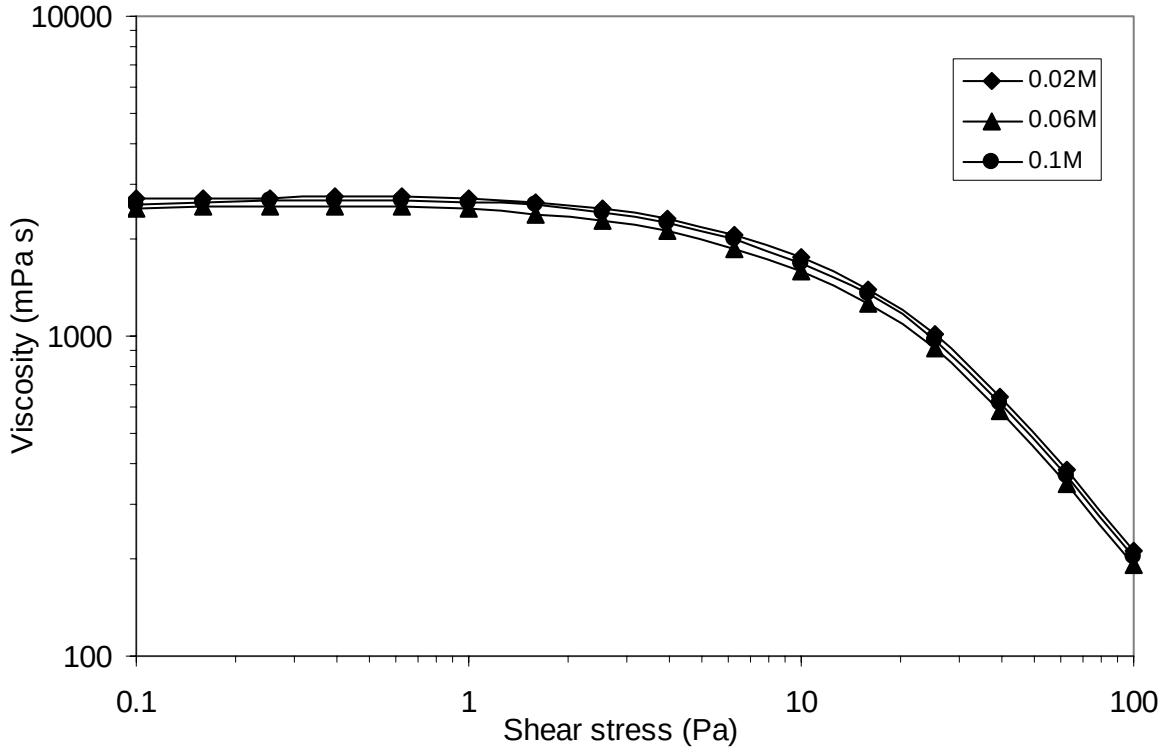

Figure 4.9: Stress dependence of the viscosity of 7wt% PADA at various sodium chloride concentrations

As mentioned above, the intermolecular hydrogen bonds play a crucial role for the network in the solution. Since the ionic strength affects the Coulomb forces, the electrostatic repulsion could be tuned by adjusting the salt concentration. However, the

variation of electrostatic interactions by changing the salt concentration appears to have a relatively small effect on the solution viscosity. . This interesting behavior could be explained by competition between two opposing trends. The weakened repulsion due to high ionic strength can facilitate intermolecular association, but in the meantime results in contraction of polymer chains, lowering the viscosity. Because there is a slight decrease in the viscosity as shown in Figure 4.9, the effect of chain contraction appears to be stronger.

4.1.3 PADA mixed with surfactant vesicles

The effects of surfactant SDBS/LSB vesicles on the rheological behaviors of PADA solutions at 7wt% and 5wt% were examined.

The steady state viscosity of 7wt% PADA solution was shown as a function of shear stress at various concentrations of vesicles in Figure 4.10. It is clearly seen that the trend of the flow curves is rather similar. At low stress, there was a Newtonian region followed by the shear-thinning zone, no matter whether vesicles were added or not. The vesicle effect on the flow curve for 5wt% PADA solution is similar to that of 7wt% solution, as shown in Figure 4.11. Figure 4.12 shows the zero-shear viscosity for 7wt% PADA solution as a function of vesicle concentration. The variation of the zero-shear viscosity with the vesicle concentration is not monotonic. At low vesicle concentrations, the zero-shear viscosity is reduced, while it is enhanced by vesicles at higher concentrations. Compared to 7wt% pure PADA solution, the solution mixed with 7mM surfactant (vesicles) has higher zero-shear viscosity, which increases by 40% at most (3800mPas vs. 2700mPa s).

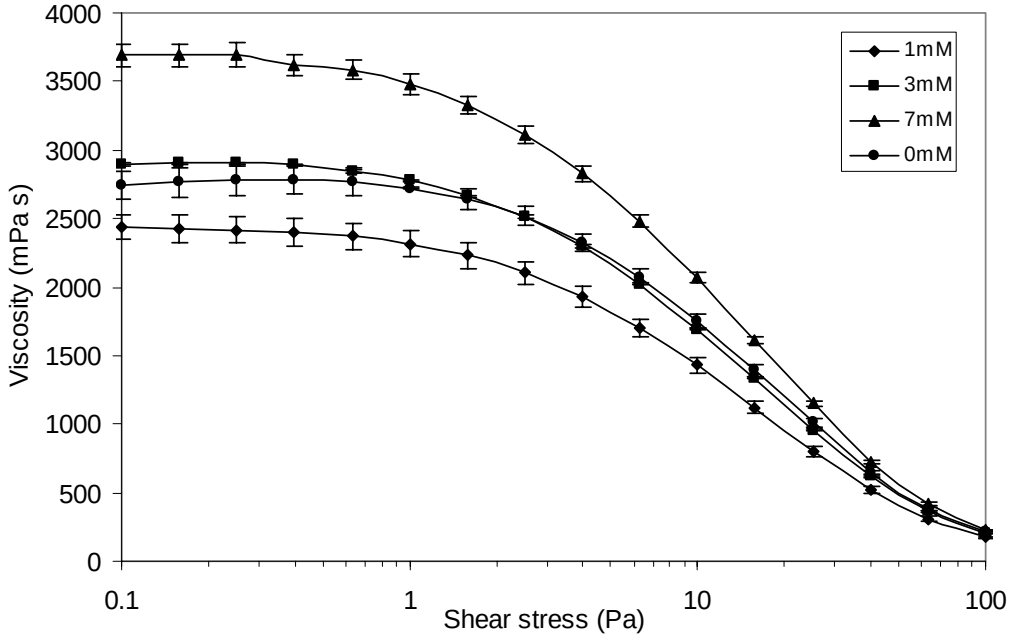

Figure 4.10: Stress dependence of the viscosity of 7wt%PADA mixed with vesicles at various concentrations

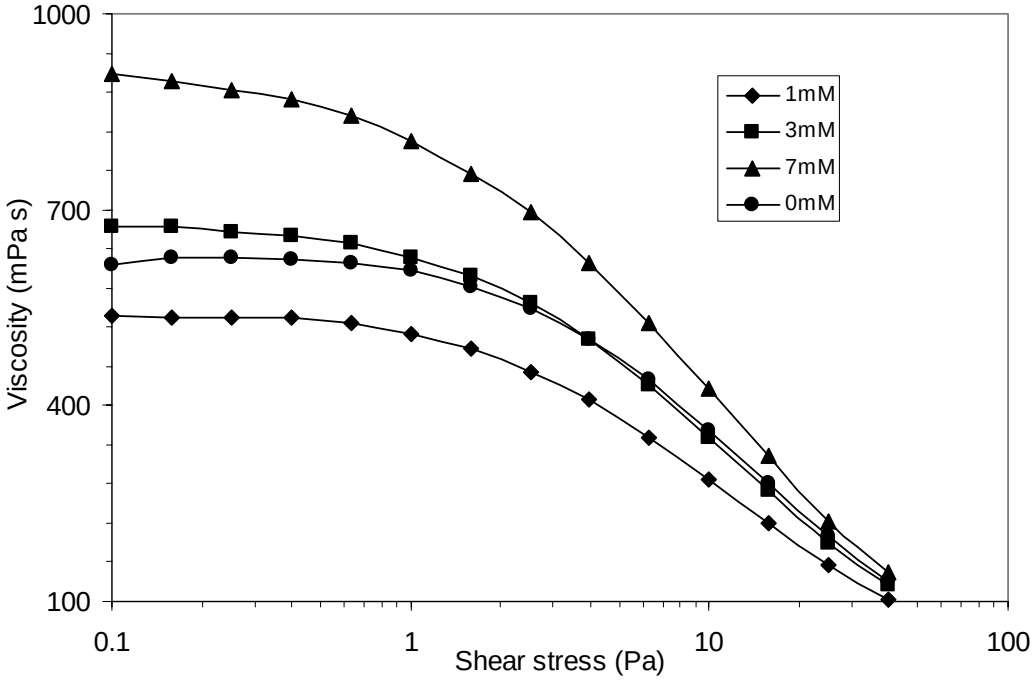

Figure 4.11: Stress dependence of the viscosity of 5%PADA mixed with vesicles at various concentrations

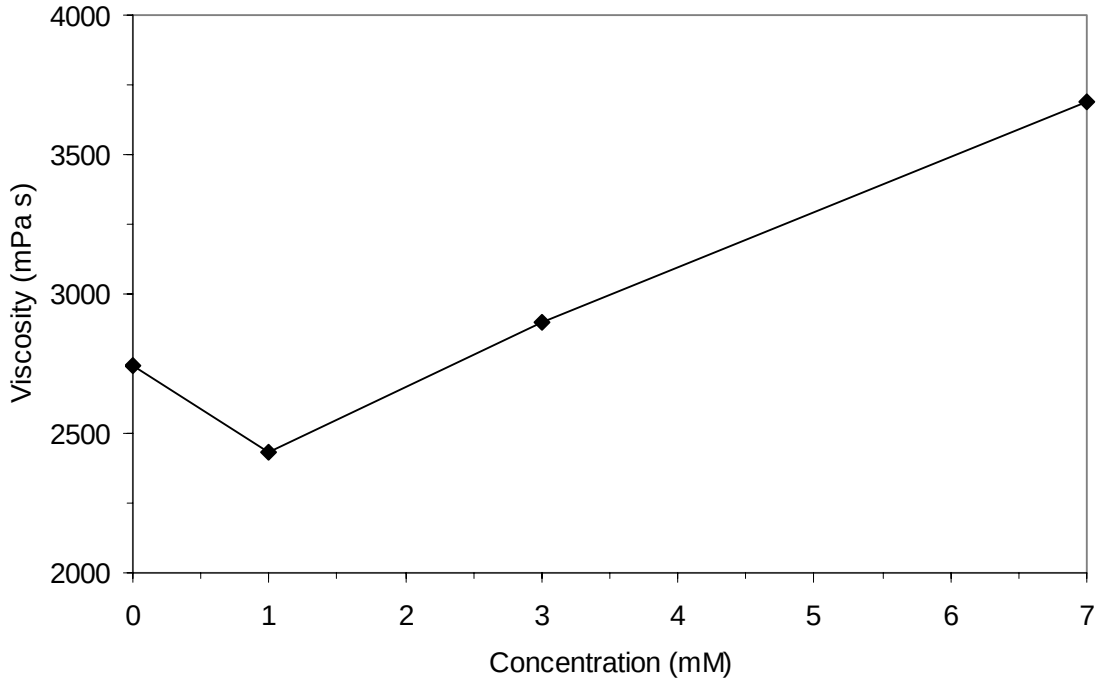

Figure 4.12: Zero-shear viscosity of 7wt% PADA solution as a function of surfactant concentration

As discussed above, the pure 7wt% PADA solution lies in the concentrated regime. When negatively charged vesicles were introduced into the solution, the positively charged copolymer PADA adsorbed on the surface of vesicles. Due to excess of PADA, it was reasonable to be assumed that more polymers adsorbed on the vesicle surface than what was needed to neutralize its original charge, leaving the polymer-coated vesicle positively charged (charge reversal). Compared to the pure PADA solution, the polymer solutions mixed with vesicles might have different networks. On one hand, the polymer adsorbing on the surface of vesicles probably reduced the cross-links, weakening the networks. On the other hand, the polymer-coated vesicles likely served as new cross-links, enhancing the networks. Whether the networks were weakened or enhanced depended on the two opposing effects. If the enhancing effect was larger, the networks

would be enhanced; if the weakening effect was larger, the networks would be weakened; if the effects were comparable to each other, the networks would be similar to that of the pure PADA solution. The viscosity depended on the network strength. Perhaps, at the vesicle concentration 3mM, the weakening effect is offset by the reinforcing one.

According to results obtained here, at low vesicle concentration, the viscosity of mixtures was lower than the pure PADA solution. This means that at low vesicle concentration, the network was impaired. The formed new cross-links may not be sufficient to compensate those destroyed due to the adsorption of the polymer on the surface of vesicles. The situation changed with increasing vesicle concentration. The viscosity gradually increased to exceed that of the pure polymer solution. It seemed that the new cross-links could make up and surpass the destroyed ones.

The Figure 4.13 presents typical results of the storage modulus *G'* and of the loss modulus *G''* as a function of frequency. As shown in Figure 4.3, the mechanical spectra could not be fitted to a one-mode Maxwell model, because there is a distribution of relaxation times.

For a one-mode Maxwell system, a crossover point, if any, is one where the storage modulus *G'* cross the loss modulus *G''* in a frequency sweep test. At the crossover point, the modulus is called crossover modulus, and the frequency is referred to crossover frequency. The crossover modulus has an important physical meaning. It directly relates to the number of cross-links (cross-link density). The higher the crossover modulus, the greater the number of cross-links is.

To analyze the data, the crossover points were used to characterize the mechanical spectra. According to the points, one can obtain crossover moduli and apparent relaxation times ($1/2\pi f_c$, where f_c is the crossover frequency). It should be noted that these two quantities have no clear physical meaning because a broad distribute of relaxation times exist in the systems. Here they only are employed to indicate how the mechanical spectra change with vesicle concentration. Figure 4.14 shows the variation of the crossover modulus with vesicle concentration. Figure 4.15 indicates concentration dependence of the apparent relaxation time. The trends are similar to that of the zero-shear viscosity. At low vesicle concentrations, both the crossover modulus and the apparent relaxation time decreased, while they were enhanced at higher concentrations. It should be noted that their variation is very small.

For comparison, it is reasonable to assume that changes in the crossover modulus and the apparent relaxation time reflect changes in the density and the lifetime of cross-links. It is noteworthy that the crossover modulus at 1mM vesicle concentration is larger than at 3mM, while the apparent relaxation time at 1mM is smaller than at 3mM. A decrease in the modulus lowers the viscosity, while a slowing down of the dynamics enhances it. Since the viscosity is higher at 3mM vesicles, the overall effects of these two opposing trends appear larger than at 1mM.

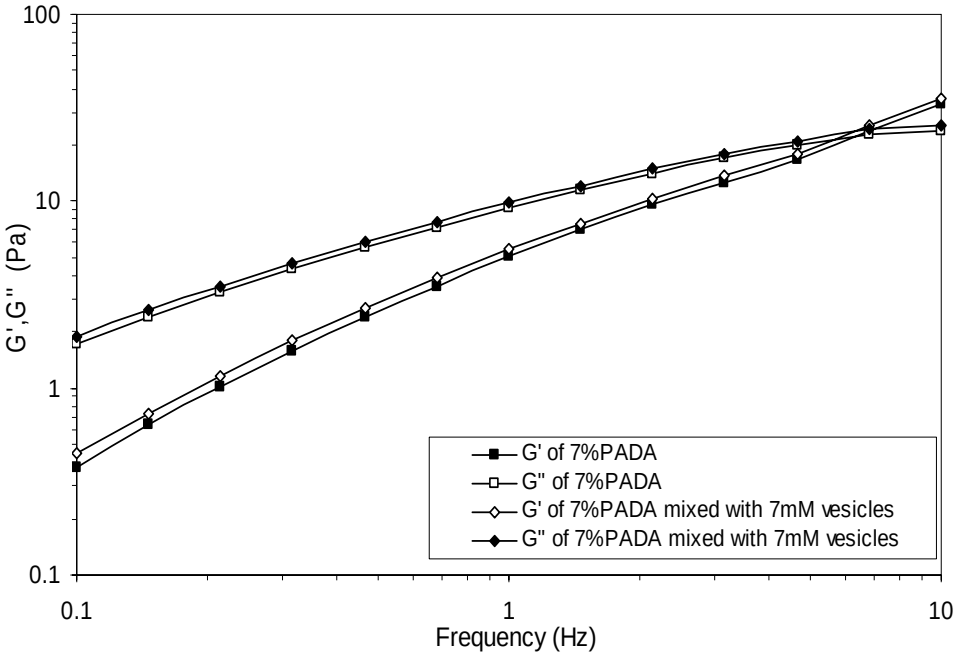

Figure 4.13: Frequency dependence of storage and loss moduli for 7wt%PADA and 7wt%PADA mixed with 7mM vesicles

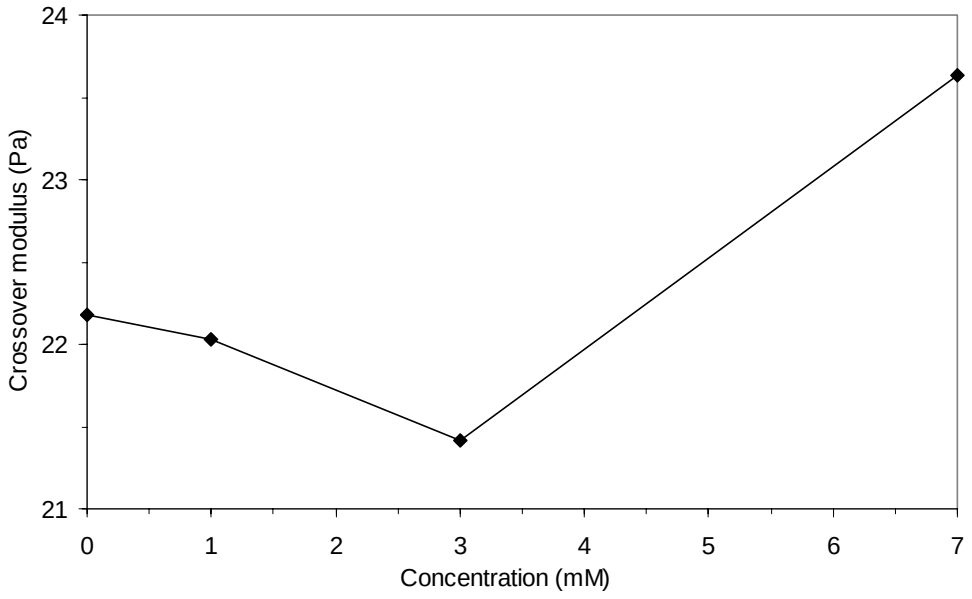

Figure 4.14: Crossover modulus versus vesicle concentration

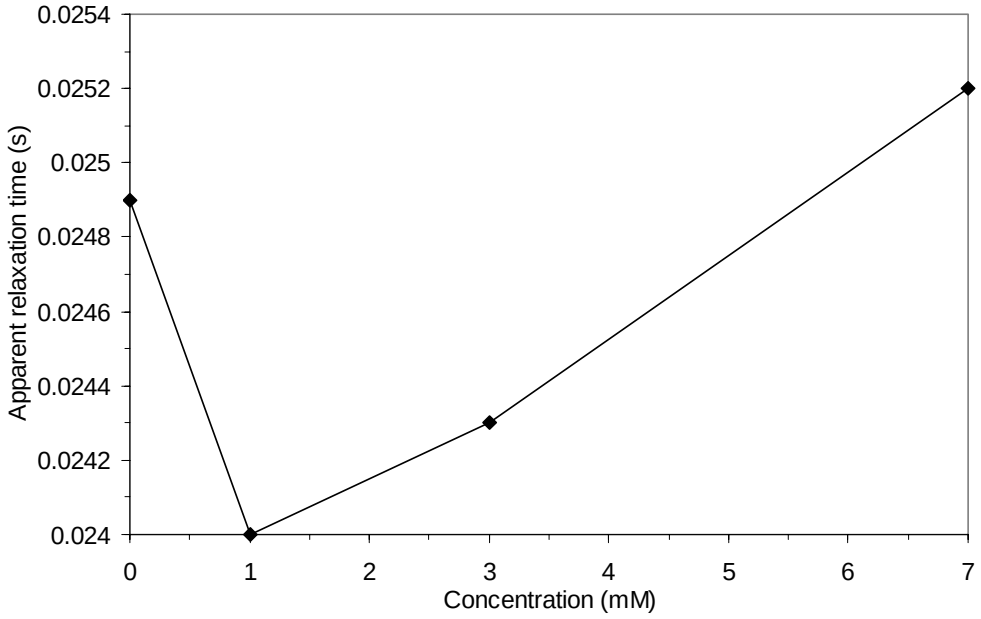

Figure 4.15: Apparent relaxation time versus vesicle concentration

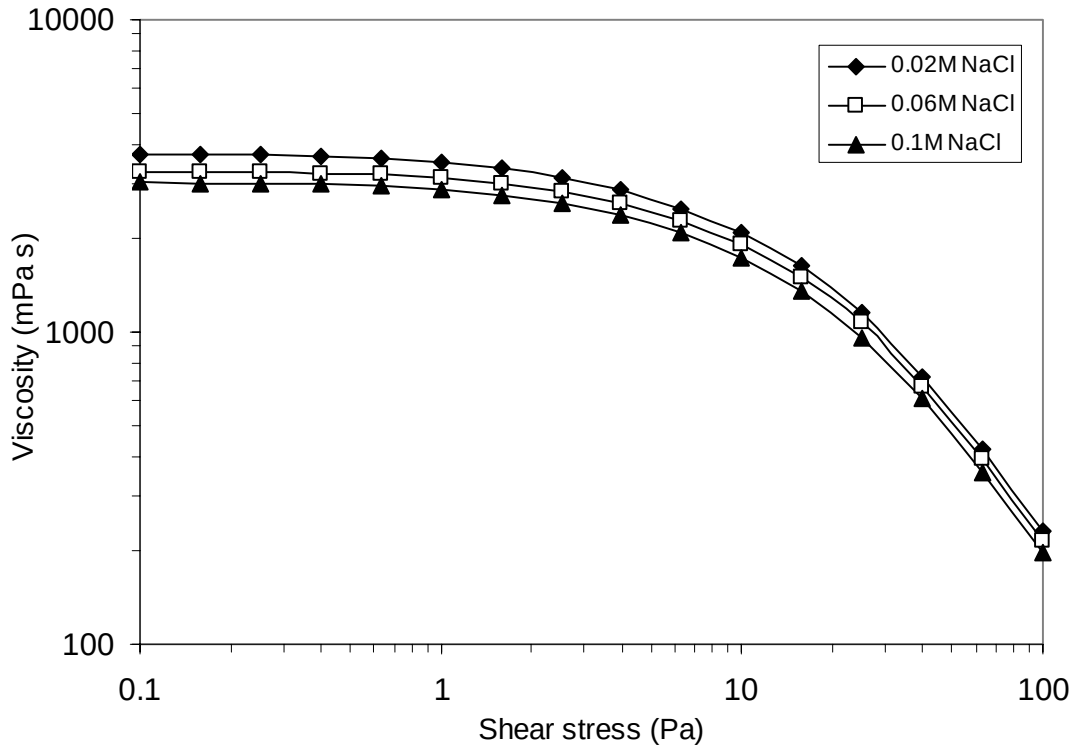

Figure 4.16: Stress dependence of the viscosity for 7wt% PADA mixed with 7mM vesicles at various salinities

The salt effect on the flow curve is shown in Figure 4.16, which plots the viscosity versus shear stress for 7wt% PADA solution mixed with 7mM vesicles at varying salt concentration. It is seen that salinity had an effect on the viscosity. Compared to the salt effect on pure 7wt% PADA solution as shown in Figure 4.9, the effect on the mixture is more pronounced. It is evident that the zero-shear viscosity decreases with salt concentration. The polymer network is affected by the electrostatic interactions that are screened by salt. On one hand, weakening the interactions between vesicles and the adsorbed polymer may result in impairing the polymer network since the polymer-coated vesicles serve as junctions. On the other hand, the repulsive forces between polymer-coated vesicles are lowered, reinforcing the network. As discussed above, weakening repulsion may promote entanglements and networking, yet result in contraction of polymer chains, unfavorable the polymer network. The latter appears stronger from the results.

4.2 hmHEC-SDBS/LSB vesicles systems

4.2.1 Phase behaviors of mixtures of hmHEC and vesicles

Table 4.2: Phase behaviors of hmHEC mixed with SDBS/LSB vesicles

Con. hmHEC [wt%] / Conc. Vesicle	0.25	0.5	1.0
0mM	●	●	●
1mM	■	■	●
2mM	■	■	—
4mM	■	—	—
5mM	■	■	●
6mM	■	■	—
8mM	■	●	●
10mM	■	●	▲
15mM	■	●	▲

Black circles represent a single-phase solution, while black rectangles signify phase separation. Black bars indicate cases that are not investigated. Black triangles stand for gel samples.

Various vesicle-polymer mixtures were examined to obtain the phase map. In this investigation, three typical phases, i.e., single-phase solution, phase separation, and gel, were observed. They were evaluated 6 days after samples were prepared. Phase separation can be identified easily by visual examination. Viscous solutions and gels can be identified by tube inversion experiments. Tube inversion is frequently used in studying gel and is basically a measure of sample yield stress (Li et al., 1997). In our experiments, vials were employed in place of test tubes. A viscous solution which has no or low yield stress will flow down in an inverted vial, while gel-like samples with sufficient yield stress will be able to hold their own weights longer than 30s.

Table 4.2 shows the phase map of hmHEC-SDBS/LSB vesicle mixtures constructed by visual examination and tube inversion. It should be noted that for comparison, the phases of the pure hmHEC in water at various concentrations were also given. As presented in Table 4.2, phase separation occurred at low polymer concentrations. At 0.25wt% hmHEC, only phase separation was observed. For 0.5wt% hmHEC, at low vesicle concentration, phase separation took place, while viscous solutions formed at higher concentration. For higher polymer concentrations like 1wt%, gel was formed with increasing the vesicle concentration. The phase separation is an associative phase separation. One phase is a concentrated solution rich in the polymer and vesicles, while the other is a water-rich phase. This is probably due to the strong hydrophobic interactions between hmHEC and SDBS/LSB vesicles, expelling the water.

4.2.2. Pure hmHEC solutions

4.2.2.1 General observations

Figure 4.17 shows typical steady state viscosities versus shear stress for three hmHEC solutions. At lower concentrations, 0.25wt% and 0.5wt%, the viscosity is approximately independent of shear stress at low shear stresses, and shear thickening occurs at intermediate shear stresses, followed by a rapid decrease at higher shear stresses. However, at higher concentration, 1wt%, the trend of the viscosity changed. There is a Newtonian plateau at low shear stresses, followed by substantial shear thinning at higher stresses. No shear thickening occurs any longer. These observations were in agreement with previous works on associative polymers (Ma and Cooper, 2001, Zhao and Chen, 2007).

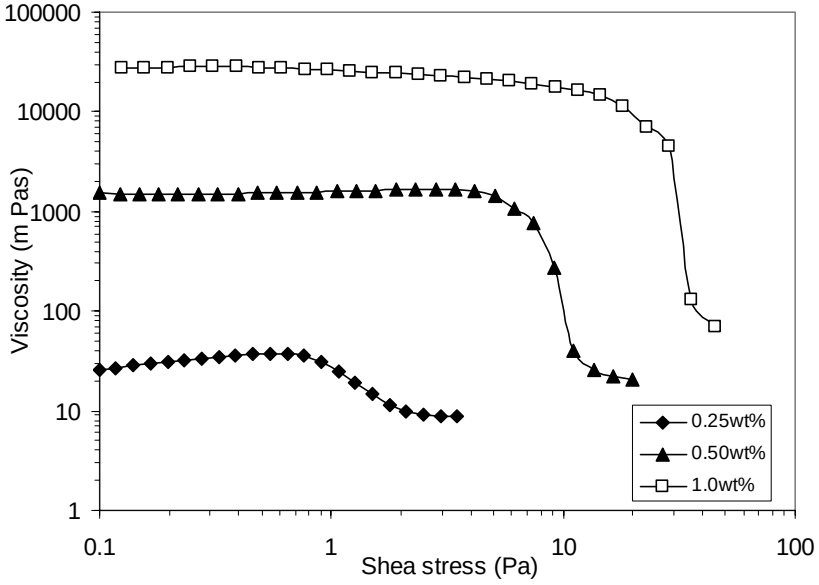

Figure 4.17: Stress dependence of the viscosity for hmHEC solutions at various concentrations

Figure 4.18 presents typical results of the storage modulus *G'* and of the loss modulus *G''* as a function of frequency for 0.5wt% hmhEC solution. At low frequency, a viscous response was observed with *G'* less than *G''*, while *G'* increases to cross *G''* at relatively higher frequency f_c , and beyond the crossover frequency, *G'* exceeds *G''*, indicating that the elastic response dominates over the viscous. The inverse of $2\pi f_c$ is often taken as the characteristic time of the system. For comparison, the calculation was made based on the simplest model of a viscoelastic fluid, the Maxwell model.

$$G' = G_\infty \frac{(f/f_c)^2}{1+(f/f_c)^2} \tag{4.7}$$

$$G'' = G_\infty \frac{f/f_c}{1+(f/f_c)^2} \tag{4.8}$$

where G_∞ is taken as G' at higher frequency. As shown in Figure 4.18, a one-mode Maxwell mode1 was not able to describe the experimental data. This observation is in agreement with the previous works (Karlson et al., 2000, Svanholm et al., 1997). Substantial deviations appeared. At low frequency, there is a smaller slope, less than 2 fore *G'*, and less then 1 for *G''*, and around the crossover, more gradual changes were observed. These indicate a distribution of relaxation times, unlike telechelic polymers which is well characterized by the Maxwell model (Lu et al., 2002). The similar linear viscoelastic behavior in Figure 4.18 is observed for most of hmHEC solutions at various concentrations investigated.

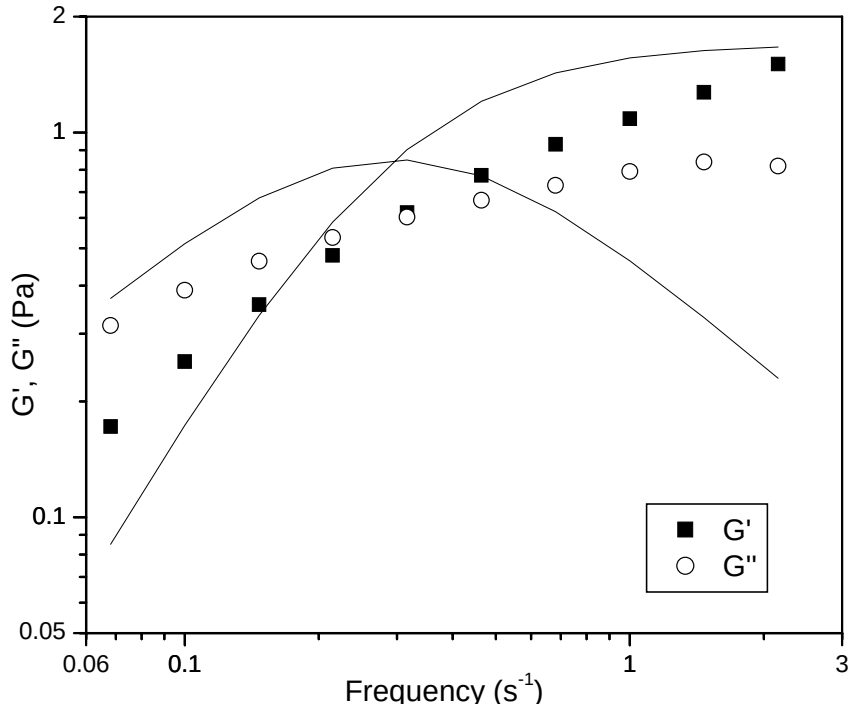

Figure 4.18: Frequency dependence of *G'* and *G''* for 0.5wt% hmHEC solution. The lines are the fits to a one-mode Maxwell model (G_∞ =1.7Pa, relaxation time=0.296s).

For many polymer solutions and melts, the relation between steady state flow curves and linear viscoelastic data are well described by the Cox-Merz rule (Cox and Merz, 1958): the steady state shear viscosity as a function of shear rate is equivalent to the complex viscosity as a function of angular velocity. This empirical rule shows that the relationship between non-linear and linear viscoelastic properties exists. One can use it to estimate the shear viscosity from dynamic measurements, and vice versa. However, the Cox-Merz rule is usually not reliable for complex structured fluid (Larson, 1999).

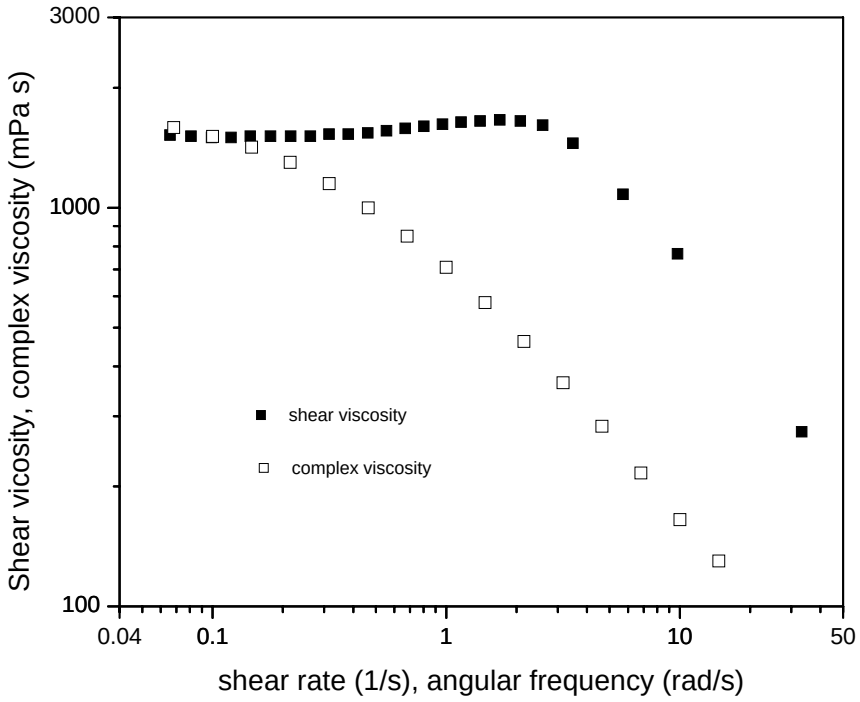

Figure 4.19: Steady state viscosity and dynamic complex viscosity versus shear rate or frequency for 0.5wt% hmHEC

The comparison between shear viscosity and complex viscosity for associative polymer hmHEC was given in Figure 4.19. It shows that the Cox-Merz rule does not hold well. The shear viscosity coincides with the complex viscosity in the Newtonian region at low shear rate or angular frequency, while at higher shear rate or angular frequency the shear viscosity deviates significantly from the complex viscosity. This is probably due to the effect of shear flow on intermolecular associations. Therefore steady state shear flow experiments are very limited to predict the viscoelastic properties. Perhaps, one can only get qualitative trends. It is noteworthy that even at higher concentrations like 1wt% where only the typical shear thinning is observed, as shown in many unmodified polymers, there still is some effect of shear flow on the intermolecular associations because the Cox-Merz rule fails.

4.2.2.2 Concentration regimes

It is important to evaluate the various concentration regimes of hmHEC solutions prior to discussion on the linear and non-linear rheological properties. For the associative polymers such as hmHEC studied here, four distinct states of solutions can be identified The four states of solutions are: dilute solution, semidilute unentangled solution, semidilute entangled solution, and concentrated entangled solution. Steady state shear experiments allow one to explore and determine these as illustrated in Figures 4.20 and 4.21.

(i) Dilute regime

For strong associations through the hydrophobes, small micelle-like aggregates via intramolecular bonding form just at a few ppm of hmHEC (Maestro et al., 2002). Beyond a threshold concentration, intermolecular associations take place. This formation of intermolecular bridges identifies the transition from the dilute to semidilute regimes. The critical concentration C_1 is probably in the vicinity of the overlap concentration of the unmodified polymer. As shown in Figure 4.21, this critical concentration is about 0.15wt% in good agreement with the previous work (Maestro et al., 2002). In the dilute regime (<0.15wt %), the zero-shear viscosity increases with concentration as $\eta_0 \sim C^{0.77}$.

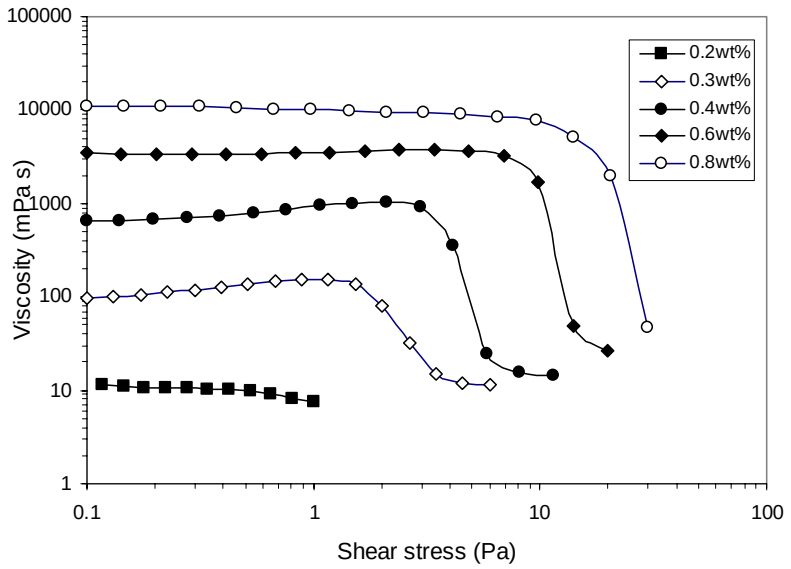

Figurge 4.20: Stress dependence of the viscosity for hmHEC solutions at various concentrations

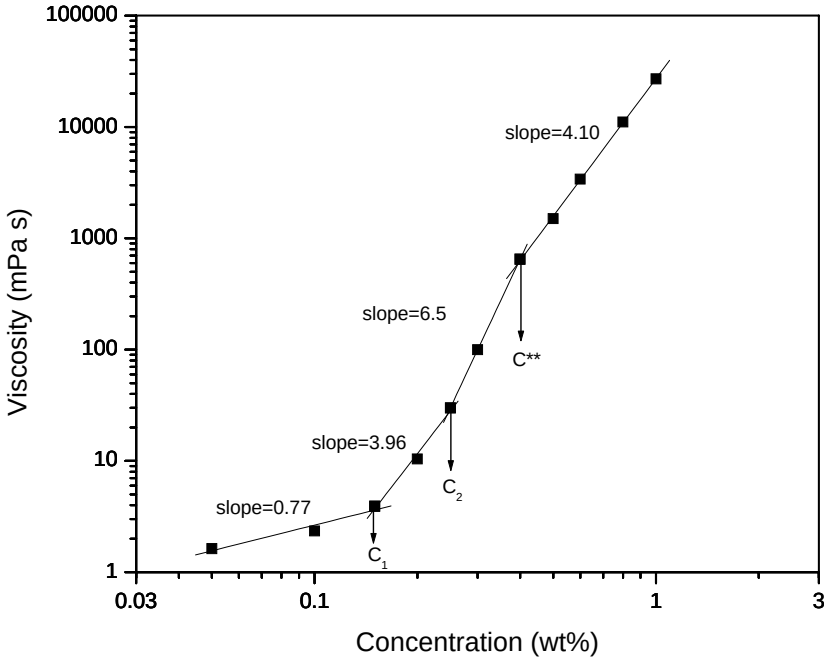

Figurge 4.21: Concentration dependence of the zero-shear viscosity for hmHEC solutions at various concentrations

(ii) Semidilute unentangled regime

Above 0.15wt%, η_0 increases more strongly ($\eta_0 \sim C^{3.96}$) until the concentration reaches C_2 (0.25wt %). The shear thickening followed by shear thinning was observed. In this regime, the intermolecular bridges take place, and are the main cause of increase in the viscosity, according to a mechanism similar to that observed with the telechelic associative polymers (Larson, 1999).

(iii) Semidilute entangled regime

Above C_2, the zero-shear viscosity follows a different scaling behavior ($\eta_0 \sim C^{6.5}$) until C** (0.4wt %) occurs. The behavior of shear thickening was observed too. The viscosity increases faster with concentration in this regime than the semidilute unentangled regime. The faster increase in the viscosity is attributed to the intermolecular associations and entanglements. The density of entanglements rises substantially until it becomes much larger than that of intermolecular associations in the regime.

(iv) Concentrated entangled regime

Above C**, the zero-shear viscosity scales as 4.1 with concentration ($\eta_0 \sim C^{4.1}$). This is probably due to entanglements which prevailing in this regime. Slight shear thickening still was observed at lower concentrations (0.5wt% and 0.6wt %), while at higher concentrations (0.8wt% and 1.0wt %) it disappeared completely.

4.2.2.3 Discussion on rheological properties

Steady state shear-flow curves and mechanical spectra at various concentrations studied were obtained. These experimental data will be discussed as follows.

(i) $C<C_1$. The viscosity is independent of the shear stress. In this dilute regime, aggregates of hmHEC are nearly isolated and no network structure is formed, and hence the system exhibits a Newtonian behavior. Compared to that of the corresponding unmodified polymer, the viscosity is slightly lower, which was deduced from the reduced viscosity (Maestro et al., 2002). This is due to the fact that intramolecular associations result in the chain contraction (Hill et al., 1993). The viscoelastic behavior of associative polymers such as hmHEC studied shows up in the semidilute regime, where intermolecular associations form.

(ii) $C_1<C<C_2$. In the semidilute unentangled regime, the intermolecular associations form through the hydrophilic chains to link adjacent aggregates, a mechanism similar to the loop-to-bridge transition for telechelic polymers (Larson, 1999). In this regime, one of remarkable features is the occurrence of shear thickening. Witten and Cohen attributed shear-thickening in polymer with multiple stickers to a shear-induced transition from intra- to intermolecular associations (Witten and Cohen, 1985). Marrucci et al. (1993) explored the possibility of shear thickening, and proposed a shear-induced non-Gaussian chain stretching effect. In the semidilute unentangled regime where both intra- and intermolecular associations exist, it seems reasonable to state that a shear-induced change in the balance between intra- and intermolecular associations is the

cause of the shear thickening. English et al. showed evidence of a shear-induced structuring associated with shear thickening at low polymer concentrations for hydrophobically modified alkali-soluble emuslsion. (English et al., 1997) At low concentrations, many of the hydrophobic associations are intramolecular. At low shear stress, the intramolecular associations contribute little or nothing to the viscosity. Upon further increasing shear stress, the polymer molecules are stretched, which makes intermolecular associations more probable and thus results in an increase in the viscosity.

The shear thickening varies with concentration. As shown in Figures 4.17 and 4.20, the shear thickening at 0.25wt% is much more pronounced than at 0.2 wt%. It is expected that the number of the intermolecular associations increases fast with concentration in this regime. In addition to, it appears that the higher the concentration, the higher the probability of the shear-induced intermolecular associations. As to the shear thinning following the shear thickening, it is probably related to the fact that at relatively high stress, shear forces become sufficient to destroy the intermolecular associations and thus the viscosity decreases. It implies that there is a transition from inter- to intramolecular associations at high shear stress. Another interesting observation is strong concentration dependence of the zero-shear viscosity ($\eta_0 \sim C^{3.96}$) in this regime. This is due to significant increase in the number of the intermolecular associations with concentration. More importantly, for hmHEC with 10 hydrophobes studied here, the dissociation of one hydrophobe from intermolecular junctions does not permit the complete relaxation of the chain because the chain still is anchored by other junctions even in the absence of entanglements. Therefore the polymer has long relaxation times, which leads to a high

viscosity. In this regime, the viscoelasticity of the solution can be described by the disassociation of an associative sequence from a cross-link followed by Rouse relaxation (Tanaka et al., 1992).

(iii) $C_2<C<C^{**}$. In the semidilute entangled regime, the intermolecular associations prevail and the entanglements become elastically effective. The shear-induced transition from intra- to intermolecular associations no longer plays an important role in shear thickening. The shear-induced non-Gaussian chain stretching seems to be the cause of the shear thickening. Ma et al. (2001) showed that shear thickening is due to the non-Gaussian chain stretching for hydrophobically end-capped poly (ethylene oxide). It is noteworthy that shear-induced disentanglement depresses the shear thickening resulting from the non-Gaussian chain stretching. As shown in Figure 4.21, a stronger concentration dependence of the zero-viscosity ($\eta_0 \sim C^{6.5}$) was observed. This observation probably is accounted for by both intermolecular associations and entanglements.

(iv) $C>C^{**}$. In the concentrated entangled regime, the extent of entanglements is high and increases strongly with concentration. The entanglement will finally dominate over the intermolecular hydrophobic association. So the shear thickening gradually disappears, as shown in Figures 4.17 and 4.20. There still is a weak shear thickening at lower concentrations (0.5wt% and 0.6wt %), while the shear thickening is completely undetectable at higher concentrations (0.8wt% and 1.0wt %). It is noteworthy that an abrupt decline in viscosity at a critical shear stress occurs in this regime. The discontinuity is attributed to the fact that the transient network is destroyed under the critical shear stress (Aubry and Moan, 2004). For entangled networks consisting of linear

chains with temporary cross-links like the systems investigated here, the linear viscoelatic response can be described well through the sticky reptation model developed by Leibler et al. (1991).

4.2.3 hmHEC solutions mixed with surfactant vesicles

The effects of surfactant SDBS/LSB vesicles on the rheological behavior of hmHEC solutions were examined. 0.5wt% and 1.0wt% were chosen.

4.2.3.1 0.5wt%hmHEC solutions with vesicles.

The steady state viscosity of 0.5wt% hmHEC was shown in Figure 4.22 as a function of shear stress at various vesicle concentrations. Compared to the flow curve of 0.5% hmHEC solution, there are two changes for the flow curves of 0.5% hmHEC solution mixed with vesicles. One is that the shear thickening disappeared completely. Only the typical shear thinning was observed in all samples with vesicles studied here. It seems that the majority of the cross-links in the network are entanglements. The other is that all samples exhibited an enhanced viscosity, compare to pure 0.5wt% hmHEC. Figure 4.23 shows the zero-shear viscosity as a function of vesicle concentration. The variation of the zero-shear viscosity versus vesicle concentration was not monotonic. The zero-shear viscosity initially increased with vesicle concentration and reached the maximum at about 8mM. Beyond this concentration, the viscosity decreased with concentration. The viscosity maximum is about 16 times higher than that in the absence of vesicles.

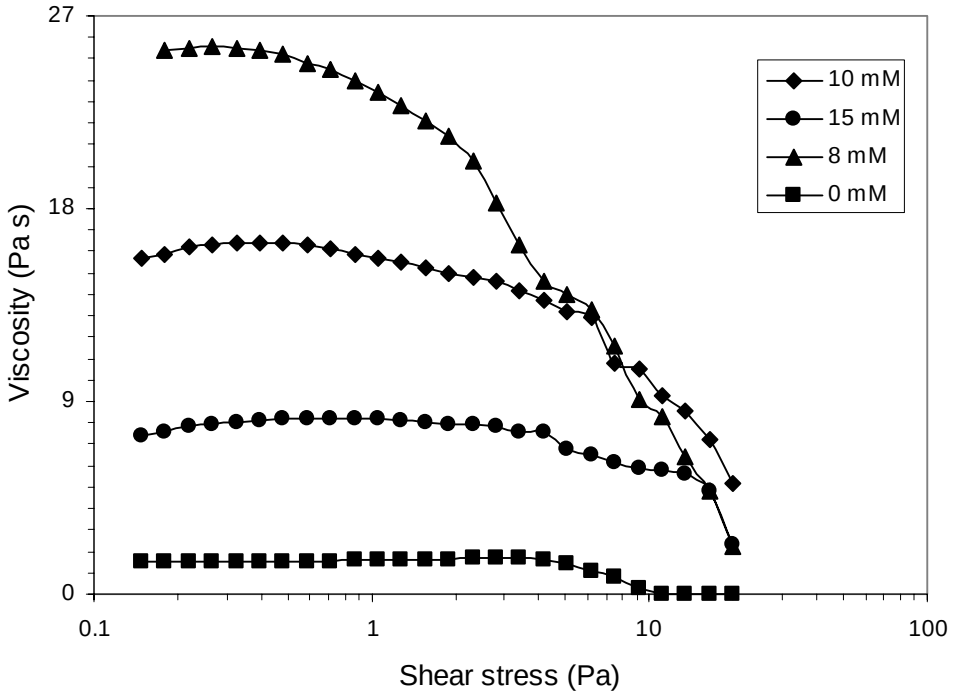

Figure 4.22: Stress dependence of viscosity of 0.5wt%hmHEC at various surfactant vesicle concentrations

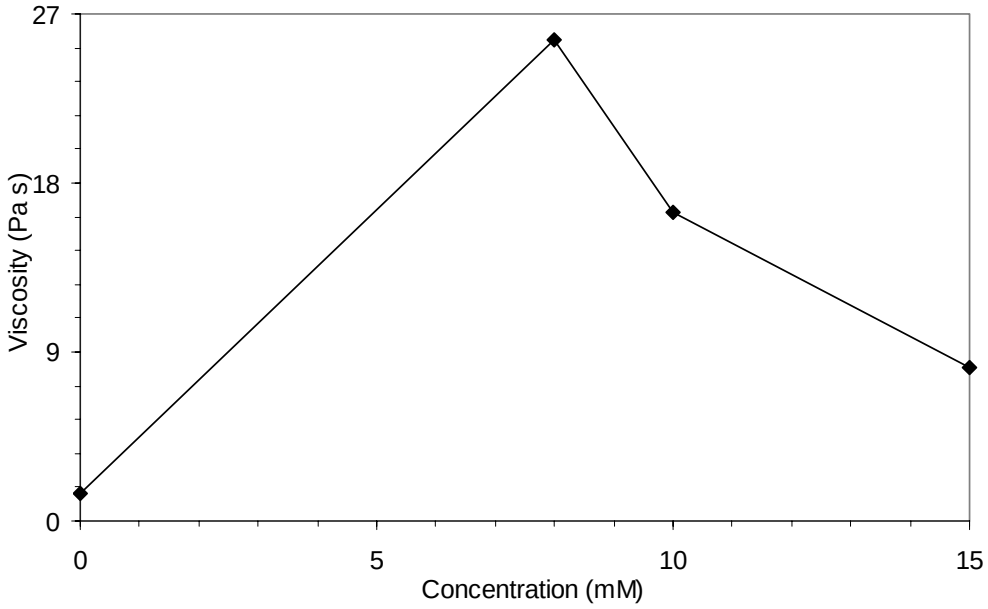

Figure 4.23: Zero-shear viscosity of 0.5 wt% hmHEC solution as a function of vesicle concentration

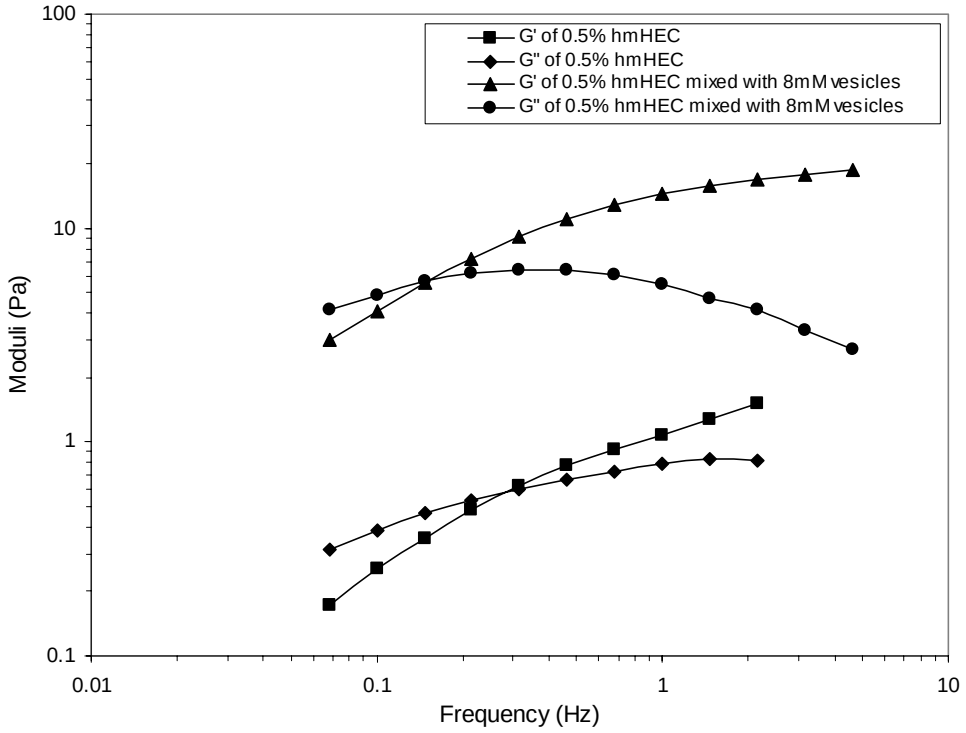

Figure 4.24: Frequency dependence of storage and loss moduli for 0.5wt% hmHEC and 0.5wt%mhHEC mixed with 8mM vesicles

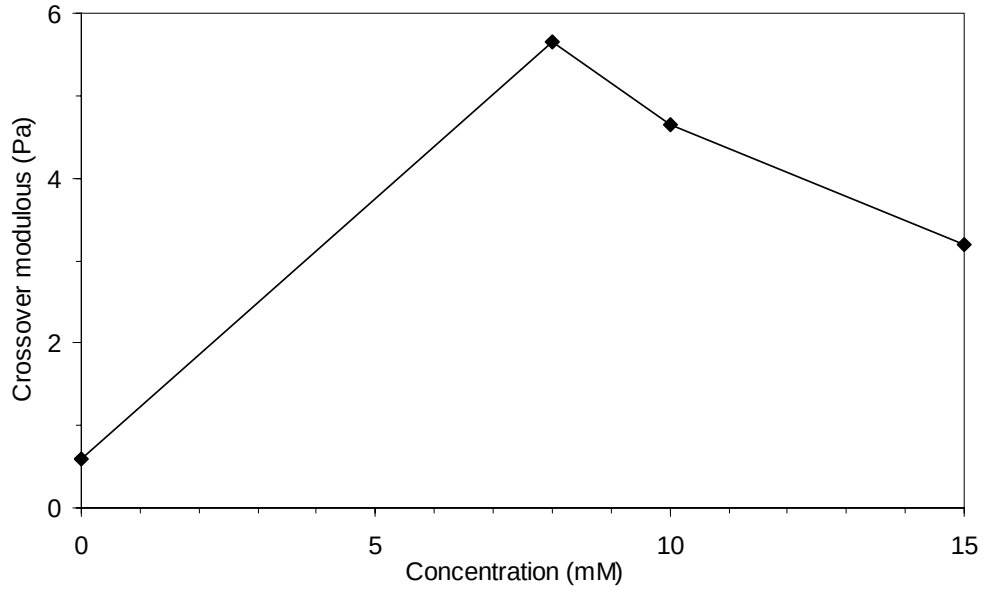

Figure 4.25: Crossover modulus versus vesicle concentration

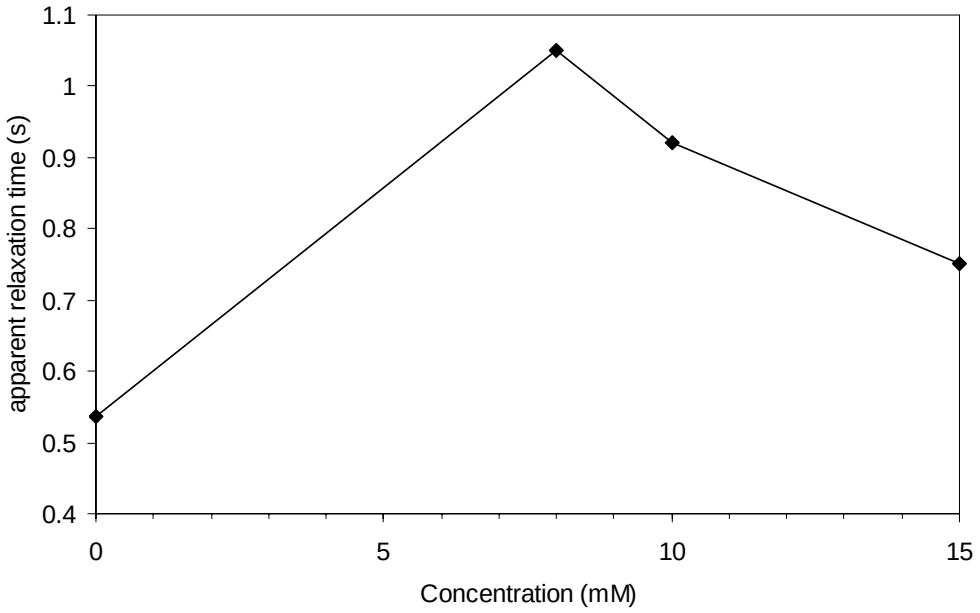

Figure 4.26: Apparent relaxation time versus vesicle concentration

The Figure 4.24 presents typical results of the storage modulus *G'* and of the loss modulus *G''* as a function of frequency. As shown in Figure 4.18, the mechanical spectra could not be fitted to a one-mode Maxwell model. In addition to, within the accessible frequency range the plateau elastic modulus at the terminal high-frequency region could not be obtained. To analyze the data, the crossover points were used to characterize the mechanical spectra again. Two characteristic quantities were the crossover modulus and the inverse of the crossover angular frequency, which may be called the apparent relaxation time (Piculell et al., 2003). Figure 4.25 shows the variation of the crossover modulus with vesicle concentration. Figure 4.26 indicates the concentration dependence of the apparent relaxation time. The trends are similar to that of the zero-shear viscosity. Both the crossover modulus and the apparent relaxation time initially increased and reached the maximum at about 8mM, followed by a decrease, unlike hmHEC mixed with

surfactant micelles where the crossover modulus decreased monotonically with concentration (Piculell et al., 2003).

To interpret these trends, it is reasonable to assert that changes in the crossover modulus and the apparent relaxation time reflect changes in the density and the lifetime of cross-links. It appears that the sample with 8mM vesicles has the largest number of cross-links and the slowest dynamics. These two cooperative factors result in the maximum in viscosity.

As discussed above, for the pure 0.5wt% hmHEC solution, intermolecular associations and entanglements coexist. When vesicles were introduced into the solution, the hydrophobic associations between vesicle and the polymer (or polymer-vesicle bonds), where hydrophobes of hmHEC anchore to the hydorophobic interior of the vesicle bilayer, dominated over the intermolecular associations among the polymer. The vesicles act as multifunctional cross-links in a three-dimensional network. In contrast to the intermolecular associations, vesicles have much bigger characteristic time scales. This means that the hydrophobe residence time is much longer, so a hydrophobe can keep anchored in a given vesicle for a long time. According to the results shown in Figure 4.26, the average lifetime of the crosslink in hmHEC solutions mixed with vesicles is longer than that in the pure hmHEC solution.

Besides the relaxation times, the density of the cross-links has to be considered. The cross-links include entanglements and effective polymer-bonds. It is rather complicated to identify the density of the cross-links. So it is still difficult to answer how

the three-dimensional network changes with vesicle concentration or the number ratio of the number of polymer chains to that of vesicles in the systems. To gain some insights, let us consider two simple imaginary scenarios. The first is that only one vesicle was added into the solution. The other is that a certain amount of vesicles were added into the solution to make one hydrophobe per vesicle. For the first scenario, theoretically the network would be enhanced. For the second one, it is probable that Cross-links would be eliminated because one vesicle only one hydrophobe. As a result, the network would be destroyed and rheological properties would be depressed greatly. In view of the much high aggregation number of a vesicle for a realistic case, the second scenario may not be realized, but it gives us some ideal of the behavior trend. The network does not monotonically vary with vesicle concentration. Therefore it is reasonable to state that in the low vesicle concentration range, the three-dimensional network is gradually enhanced with concentration, and above a critical concentration at which the polymer hydrophobes saturated with vesicles, the network begins to be weakened until it is destroyed if possible. Our observations seem to be in accordance with this interpretation.

4.3.3.2 1.0wt%hmHEC solutions with vesicles.

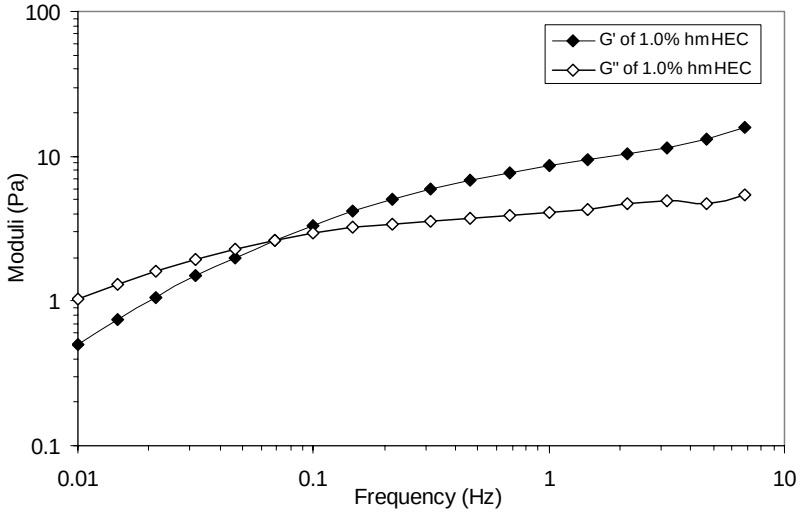

(a)

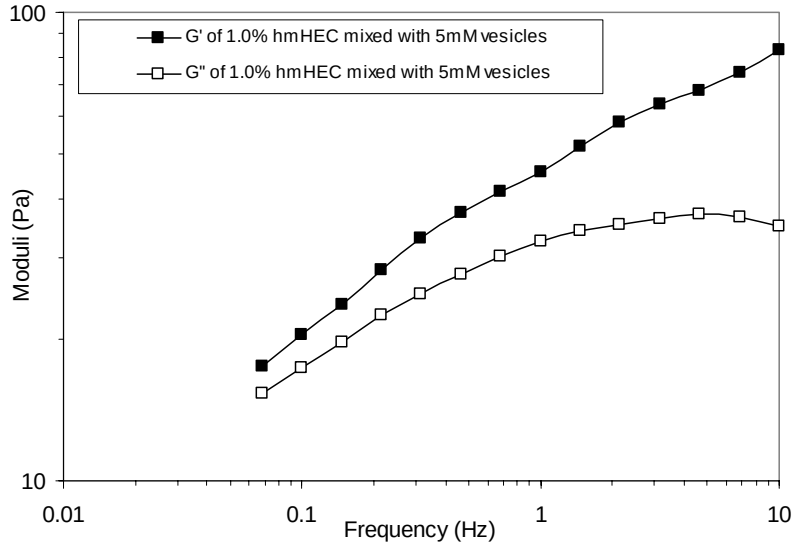

(b)

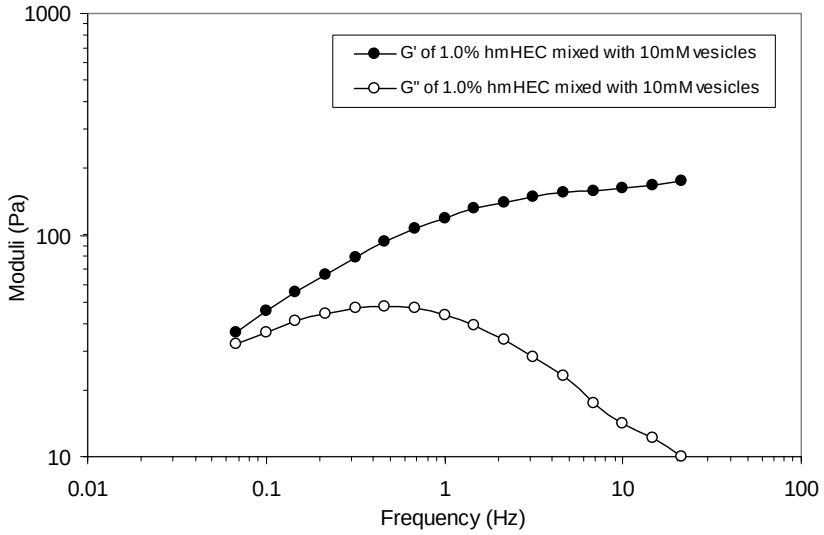

(c)

Figure 4.27: Storage modulus (*G'*) and loss modulus (*G''*) as a function of frequency for 1.0w% hmHEC mixed with vesicles at various concentration (a) 0mM, (b) 5mM, and (c)10mM.

It is interesting that the gel-like samples containing 1.0wt% hmHEC and 10mM vesicles were obtained. Dynamic measurements were employed to investigate the progression from viscous solution to gel. Representative measurements of storage and loss moduli as a function of frequency for mixtures of vesicles and hmHEC are presented in Figure 4.27. The first sample is pure 1.0wt% hmHEC solution, and the remaining two are mixtures of 1.0wt%hmHEC and vesicles with varying concentrations. The 1.0w% hmHEC solution has a crossover point in its dynamic rheological response, while the others have no crossover points within the accessible frequency range, and the storage modulus G' is greater than the loss modulus G''. It means that the two samples containing vesicles have long relaxation times. Compared to the sample with 5mM vesicles, the gel-like sample has a much higher storage modulus and tends to a plateau elastic modulus at relatively higher frequency.

Chapter 5 CONCLUSIONS

The main findings of the present research and the conclusions are summarized as follows.

5.1 PADA-SDBS/LSB vesicle systems

The phase map of the mixtures was constructed. Two typical behaviors, i.e., a solution and a phase separation into a supernatant and a precipitate were observed. Precipitation probably occurred around the isoelectric point.

For pure PADA solutions, the system is Newtonian at low concentration, while shear thinning takes place at high concentration. Intermolecular hydrogen bonds are the driving force for entanglements and network.

Different concentration regimes were identified, a dilute regime C < C*(ca. 1wt %), a semidilute regime C* < C < C** (ca. 3wt %), and a concentrated regime C >C**. In the dilute regime, polymer coils are almost isolated and hence the solution is Newtonian. Both the electrostatic interactions between cationic monomers and the intramolecular hydrogen bonds affect the viscosity. The polymer in the semidilute regime has a different scaling behavior from that in the concentrated regime. The semidilute regime is characterized by the power law $\eta_0 \sim C^{2.1}$, while the concentrated one has a scaling behavior of $\eta_0 \sim C^{4.26}$. In the semidilute regime, the intermolecular hydrogen bonds form and become strong driving forces for entanglements, whereas the electrostatic repulsive

forces resist them. According to the results, the hydrogen bonds appear to dominate over the repulsive forces. In this regime, the number of cross-links strongly increases with the concentration.

The temperature effect on the viscosity was examined. The viscosity decreases with increasing temperature. The activation energy of disentanglement is estimated to be around 13 KJ/mol, less than the strength of hydrogen bonds 21kJ/mol. This is probably attributable to the electrostatic repulsion between cationic monomers. The salt effect on viscosity was also investigated. It seemed that salinity has no pronounced effect on the flow curve.

The effects of surfactant vesicles on the viscosity and viscoelasticity of PADA solutions were examined. The variation of the zero-shear viscosity versus vesicle concentration is not monotonic. At low vesicle concentrations, the zero-shear viscosity is weakened, while it is enhanced by vesicles at higher concentrations. An analysis of the oscillatory shear data for the vesicle-polymer samples showed that added surfactant vesicles affected both the lifetime and the structure of the transient PADA-vesicle network, due to adsorption of PADA on the surface of the vesicles. At low vesicle concentrations, both the crossover modulus and the apparent relaxation time decreased, while they were enhanced at higher concentrations. It is noteworthy that added salt has a significant effect on the viscosity of polymer-vesicle mixtures.

5.2 hmHEC-SDBS/LSB vesicle systems

The phase map of the mixtures was constructed. Three typical behaviors, i.e., viscous solution, phase separation, and gel, were observed. The phase separation is an associative phase separation. One phase is a concentrated phase rich in the polymer and vesicles, while the other is a water-rich phase. This is probably due to the strong hydrophobic interactions between hmHEC and SDBS/LSB vesicles, expelling the water. The gel can hold its own weight upon tube inversion.

Different concentration regimes of hmHEC solutions are identified: a dilute regime (C<0.15wt %), a semidilute unentangled regime (0.15wt %< C<0.25wt %), a semidilute entangled regime (0.25wt %< C<0.4wt %), and a concentrated regime (C >0.4wt %). In the dilute regime, aggregates of hmHEC are nearly isolated and no network structure formed, and hence the system exhibits a Newtonian behavior. Compared to that of the corresponding unmodified polymer, the viscosity is slightly lower. In the semidilute unentangled regime, the intermolecular associations take place through the hydrophilic chains to link adjacent aggregates. Shear thickening starts to occur at intermediate shear rates. This is probably due to a shear-induced transition from intra- to intermolecular associations. Another interesting observation is much stronger concentration dependence of the zero-shear viscosity ($\eta_0 \sim C^{3.96}$) in this regime. It is due to a significant increase in the number of the intermolecular junctions with concentration.

In the semidilute entangled regime, the intermolecular associations prevail and the entanglements become elastically effective. The shear-induced transition from intra- to

intermolecular associations is no longer significant to result in shear thickening. The shear-induced non-Gaussian chain stretching seems to be the cause of the observed shear thickening. Shear-induced disentanglement depresses the shear thickening. A stronger concentration dependence of the zero-viscosity ($\eta_0 \sim C^{6.5}$) was observed. This observation probably is accounted for by both intermolecular associations and entanglements. In the concentrated entangled regime, the shear thickening gradually disappears. The number of entanglements is large and increases strongly with concentration. The entanglements finally dominate over the intermolecular hydrophobic associations. An abrupt decline in viscosity at a critical shear stress occurs in this regime. The discontinuity is probably attributed to the fact that the transient network is destroyed by a shear stress beyond the critical value.

The effects of vesicles on the rheological behavior of hmHEC solutions were examined. 0.5wt% and 1.0wt% were chosen. Compared to the flow curve of 0.5% hmHEC solution, there are two changes for the flow curves of 0.5% hmHEC solution mixed with vesicles. Firstly, the shear thickening disappeared completely. This is probably attributed to the fact that the majority of the cross-links in the network are entanglements. Secondly, the variation of the zero-shear viscosity with vesicle concentration was not monotonic. The zero-shear viscosity initially increased with vesicle concentration and reached a maximum at about 8mM. Beyond this concentration, the viscosity decreased with concentration. The dynamic results showed that the added surfactant vesicles affected both the lifetime and the structure of the hmHEC-vesicle network. Both the crossover modulus and the apparent relaxation time initially increased

and reached the maxima at about 8mM, followed by a decrease, unlike hmHEC mixed with surfactant micelles where the crossover modulus decreased monotonically with concentration. It may be reasonable to assume that in the low vesicle concentration range, the three-dimensional network is gradually enhanced with concentration, and above a critical concentration at which the polymer hydrophobes saturated with vesicles, the network begins to be weakened until it is destroyed if possible.

The gel-like samples containing 1.0wt% hmHEC and 10mM vesicles were obtained. Dynamic measurements were employed to investigate the transition from a viscous solution to a gel. The relaxation times are longer for higher vesicle concentrations, and the storage moduli are much higher.

In the present study, we have only investigated the phase behavior and rheological properties of the associative polymer-vesicle systems. We did not pay much attention to the microstructures. In fact, polyelectrolytes can lead to structural changes in vesicle, like formation of faceted vesicles (Marques et al., 1999). Hydrophobically modified polymers may induce the formation of smaller vesicles due to the re-organization of the original vesicles (Lee et al., 2005). Therefore, it is recommended to investigate the microstructure changes of vesicles by using scattering and microscopy techniques.

REFERENCES:

Antunes, F. E., and E. F. Marques, R. Gomes, K. Thuresson, B.Lindman and M. G. Miguel. Langmuir, 20, pp.4647. 2004.

Antunes, F. E., R. O. Brito, E. F.Marques, B. Lindman and M. G. Muguel. J. Phys. Chem. B, 111, pp.116. 2007.

Ashbaugh, H. S., K. Boon and R. K. Prud'homme. Colloid Polym. Sci., 280, pp.783. 2002.

Aubry T. and M. Moan. J. Rheol., 48, pp.379. 2004.

Bangham A.D., Standish M. M. and J. C. Watkins. J. Mol. Biol., 13, pp.238. 1965.

Berret, J.F., D. Clavet, A. Collet and M. Viguier. Curr. Opin. Colloid Interface Sci., 8, pp.296. 2003.

Brasher L.L. and E.W. Kaler. Langmuir, 12, pp.6270. 1996.

Cox, W. P. and E. H. Merz, J. Polym. Sci., 28, pp.619. 1958.

Discher, D. E. and A. Eisenberg. Science, 297, pp. 967. 2002.

Dobrynin A.V. and M. Rubinstein. Prog. Polym. Sci., 30, pp.1049. 2005.

Doi, M.and S. F. Edwards. The Theory of Polymer Dynamics, 1st ed. New York: Oxford University Press, 1986.

English, R. J., H. S. Gulati, R. D. Jenkins and S. A. Khan. J.Rheol., 41, pp.427. 1997.

Ferry, J. D. Viscoelastic Properties of Polymers. New York: John Wiley &Sons, Inc., 1980.

Herrington K.L., E.W. Kaler, D.D. Miller, J.A.N. Zasadzinski and S. Chiruvolu. J. Phys. Chem., 97, pp.13792. 1993.

Hiemenz P.C. and R. Rajagopalan. Principles of colloid and surfaces chemistry. New York: Marcel Dekker, Inc., 1997.

Hill, A., F. Candau and J. Selb. Macromolecules, 26, pp.4521. 1993.

Israelachvili, J. N. Intermolecular and Surface Forces. New York: Academic Press, 1992.

Kaler, E. W., A. K. Murthy, B. E. Rodriguez and J. A. N. Zasadzinski. Science, 245, PP.1371. 1989.

Karlson, L., F. Joabson and K. Thuresson. Carbohydr. Polym., 41, pp.25. 2000.

Kevelam, J., J. F. L. vanBreemen, W. Blokzijl and J. Engberts. Langmuir, 12, pp.4709. 1996.

Kondo Y., H. Uchiyama, N. Yoshino, K. Nishiyama and M. Abe. Langmuir**,** 11, pp.2380. 1995.

Kulicke W. M. and R. S. Porter. Rheol. Acta, 19, pp.601. 1980.

Kulicke W. M. and R. Kniewske. Makromol. Chem., 182, pp.2277. 1981.

Larson, R. G. The Stucture and Rheology of Complex Fluids. New York: Oxford University Press, 1999.

Lasic, D. D. Liposomes: From Physics to Applications. Amsterdam: Elsevier, 1993.

Lee, J.H., J. P. Gustin, T. H.Chen, G. F. Payne and S. R. Raghavan. Langmuir, 21, pp.26. 2005.

Leibler, L., M. Rubinstein and R. H. Colby. Macromolecules, 24, pp.4701. 1991

Li, H., G.E. Yu, C. Price, C. Booth, E. Hecht and H. Hoffmann, Macromolecules, 30, 1347. 1997.

Lin, C. C., C. H. Chang and Y. M. Yang. Colloids Surf. A, 346, pp.66. 2009.

Loyen, K., I. Iliopoulos, R. Audebert, and U. Olsson. Langmuir, 11, pp.1053. 1995.

Lu, Q. and M. J. Solomon, Phys. Rev. E., 66, 061504. 2002.

Ma S. X. and S. L.Cooper. Macromolecules, 34, pp.3294. 2001.

Maestro, A., C. Gonzalez and J. M. Gutierrez, J. Rheol., 46, pp.127. 2002.

Mark, J.,et.al., Physical Properties of Polymers. Washington, D.C.: American Chemical Society, 1984.

Marques E.F., O. Regev, A. Khan, M. G. Miguel and B. Lindman. J. Phys Chem. B, 102, pp.6746. 1998.

Marques, E. F., O. Regev, A. Khan, A. Miguel and B. Lindman. Macromolecules, 32, pp.6626. 1999.

Marques, E.F., O. Regev, A. Khan and B. Lindman. Adv. Colloid Interface Sci., 100-102, pp.83-104. 2003.

Marrucci, G., S. Bhargava and S. L. Cooper. Macromolecules, 26, pp.6483. 1993.

Meagher R.J., T.A. Hatton and A. Bose. Langmuir, 14, pp.4081. 1998.

Medronho, B., F. E. Antunes, B. Lindman and M. G. Miguel. J. Dispers. Sci. Tech., 27, pp.83. 2006,

Meier, W., J. Hotz and S. GuntherAusborn. Langmuir, 12, pp.5028. 1996.

Murphy, A., A. Hill and B. Vincent. Ber. Bunsen-Ges. Phys. Chem. Chem. Phys., 100, pp.963. 1996.

O'Connor A.J., T.A. Hatton and A. Bose. Langmuir, 13, pp.6931. 1997.

Piculell L., M. Egermayer and J. Sjostrom. Langmuir, 19, pp.3643. 2003.

Regev, O., E. F. Marques and A. Khan. Langmuir, 15, pp.642. 1999.

Salkar R.A., D. Mukesh, S.D. Samant and C. Manohar. Langmuir, 14, pp.3778. 1998.

Santos T. D., B. Medronho, F. E. Antunes, B. Lindman and M. Miguel. Colloids Surf. A, 319, pp.173. 2008.

Šegota S.and D. Težak. Adv. Colloid Interface Sci., 121, pp.51. 2006.

Svanholm, T., F. Molenaar, and A. Toussaint. Prog. Org. Coat., 30, pp.159. 1997.

Tanaka, F.and S. F. Edwards. Macromolecules, 25, pp.1516. 1992.

Tanford C. J. Phys Chem, 76, pp.3020. 1972.

Tondre, C., and C. Caillet. Adv. Colloid Interface Sci., 93, pp.115. 2001.

Viseu, M. I., E. Katarina, S. C. Claudia and M. B. C. Silva. Langmuir, 16, pp.2105. 2000.

Witten, T. A.and M. H. Cohen. Macromolecules, 18, pp.1915. 1985.

Yaacob I.I. and A. Bose. J. Colloid Interface Sci., 178, pp. 638. 1996.

Yatcilla M.T., K.L. Herrington, L.L. Brasher, E.W. Kaler, S. Chiruvolu and J.A.N. Zasadzinski. J. Phys. Chem., 100, pp.5874. 1996.

Zhai, L., G. Li and Z. Sun. Colloids Surf. A, 190, pp.275. 2001.

Zhai, L., X. Lu, W. Chen, C. Hu and L. Zheng. Colloids Surf. A, 236, pp.1. 2004.

Zhai L., M. Zhao, X. Tan, T. Li and D. Wang. J. Dispers. Sci. Tech., 26, pp.753. 2005.

Zhai L., M. Zhao, D. Sun, J. Hao and L. Zhang. J. Phys. Chem. B, 109, pp.5627. 2005.